

Review Article

# A comprehensive review on pit thermal energy storage: Technical elements, numerical approaches and recent applications



Yutong Xiang <sup>a</sup>, Zichan Xie <sup>a,b</sup>, Simon Furbo <sup>a</sup>, Dengjia Wang <sup>c</sup>, Meng Gao <sup>a</sup>, Jianhua Fan <sup>a,\*</sup>

<sup>a</sup> Department of Civil Engineering, Technical University of Denmark, Bovej 118, Kgs. Lyngby DK 2800, Denmark

<sup>b</sup> Department of Mathematics and Systems Analysis, Aalto University, School of Science, P.O. BOX 11100, Aalto, Finland

<sup>c</sup> State Key Laboratory of Green Building in Western China, Xi'an University of Architecture and Technology, Xi'an, Shaanxi 710055, China

ARTICLE INFO

**Keywords:**

Pit thermal energy storage  
Recent applications  
Floating cover  
Liner and insulation material  
Simulation approaches

ABSTRACT

Pit thermal energy storage (PTES) is one of the most promising and affordable thermal storage, which is considered essential for large-scale applications of renewable energies. However, as PTES volume increases to satisfy the seasonal storage objectives, PTES design and application are challenged. These difficulties triggered an interest in PTES investigations. This paper aims to identify the success factors and research gaps of PTES by an up-to-date evaluation of 160 recent publications. Existing technical elements that affect PTES thermal properties inclusive geometry design, inlet/outlet design, cover design, and materials, are outlined in depth. Numerical studies are categorized in terms of their mathematical theory and research purposes for a systematic discussion. The current application status of PTES systems worldwide is summarized from four aspects: storage material, geological design, operation strategy, and storage duration. For projects in operation, special attention is given to gathering and comparing operational data on solar fraction, storage efficiency, storage cycle, and PTES temperature. This review outlines the progress and potential directions for PTES design and numerical studies by identifying the research gaps that require further effort.

## 1. Introduction

Buildings account for approx. 40 % of the world's annual energy consumption. The operations of buildings, including ventilation, heating, and cooling, have the highest energy demand for buildings. However, the heating market is still dominated by fossil fuel-based equipment and less efficient traditional electric heating products, accounting for nearly 80 % of new sales [1]. As a result, the transformation of the heating industry must be accelerated to meet the climate and energy goals.

As the most sustainable energy source at present, solar thermal can cover the heating demand of buildings. Many countries have taken active and effective measures to increase the applications of solar heating systems. Solar heating systems can be divided into two categories: solar heating systems for individual buildings (i.e., small and medium scale) and solar heating systems for a group of buildings via a thermal grid (i.e., large-scale) [2]. Large-scale solar heating systems perform better than small-scale systems in terms of system efficiency and energy cost. Therefore, the number of large-scale systems has grown significantly over the past decade, especially outside Europe (as shown

in Fig. 1 [3]) [4]. By the end of 2020, there are approximately 470 solar district heating systems ( $>350 \text{ kW}_{\text{th}}$ ;  $500 \text{ m}^2$ ) in operation worldwide.

However, solar thermal energy faces challenges in terms of stability and reliability, as it is intermittent. In this context, the integration of thermal energy storage into solar heating systems has been proposed to address these challenges [5,6]. Thermal energy storage can be classified into diurnal thermal energy storage (DTES) and seasonal thermal energy storage (STES) [5,7,8] according to the energy storage durations. Nevertheless, STES systems are often seen as challenging from a technical point of view. The requirement for large capacities for seasonal storage continues to drive up the construction STES systems. Fisch et al. [9] found that solar district heating systems with STES could deliver 50–70 % of the yearly demand, whereas those with DTES could only provide 10–20 % of the annual demand, demonstrated explicitly by summarizing twenty-seven large-scale solar district heating systems. The benefit of STES systems has also been shown in terms of solar fraction (defined as the percentage of the total thermal load satisfied by solar energy) [2,10–12], where utilizing STES could increase the solar fraction from 5–15 % to 25–50 % compared to using DTES. Therefore, STES is an effective way to improve the efficiency of large-scale solar district heating systems [13].

\* Corresponding author.

E-mail address: [jifa@dtu.dk](mailto:jifa@dtu.dk) (J. Fan).

## Nomenclature

AL	aluminum
ATES	aquifer thermal energy storage
BTES	borehole thermal energy storage
DTES	diurnal thermal energy storage
ECG	expanded clay granules
EGG	expanded glass granules
EPS	expanded polystyrene
FGG	foam glass gravel
GFG	glass foam gravel
HDPE	high-density polyethylene
LDPE	low-density polyethylene
PTES	pit thermal energy storage
PE	Polyethylene
PIR	polyisocyanurate
PP	polypropylene
PUR	Polyurethane
PVC	Polyvinyl chloride
STES	seasonal thermal energy storage
SST	stainless steel
TTES	tank thermal energy storage

The best-known types of STES in a solar district heating system can be generally categorized into four categories [14–18]: tank thermal energy storage (TTES), pit thermal energy storage (PTES), borehole thermal energy storage (BTES), and aquifer thermal energy storage (ATES). The number of articles related to these four systems are illustrated in Fig. 2. Regarding these four types of STES systems, the majority of research has been done on BTES, followed by TTES, ATES, and PTES. This is because more projects for the BTES and ATES systems are undertaken as a result of the low construction costs in the early years. TTES is more flexible in geometry and less location-dependent. However, as far as we know, TTES is typically insulated with an insulating layer due to its enormous surface area [19]. Additionally, its size is constrained when TTES is built above the ground.

Although the number of PTES investigations is lower than the number of other STES, it is broadly seen that PTES system is superior to other STES systems in terms of energy density, geometry size, construction site independence, operation characteristics, and construction

costs, especially the investment costs per m<sup>3</sup> water equivalent of PTES have proven to be the lowest when the storage volume exceeds 60,000 m<sup>3</sup> [2,20]. Therefore, it has been regarded as a promising thermal storage technology in recent years due to the requirement for large storage capacity.

Since 1985, the solar district heating system with PTES has been developed and reviewed in several documents [4,13,14,16,21–24]. However, most of these papers mainly focus on general information and comparisons with other types of STES, and discussions on PTES are not in-depth. Only a few reviews are entirely relevant to PTES, including those by Novo et al. [22], Bott et al. [14], and Dahash et al. [24]. The technological basis and application status of waterproofing and thermal insulation materials were summarized [14,22]. As the key to determine the service life of PTES, comparative studies on material performance are not enough. Moreover, as constructing large-scale PTES systems tends to be costly, the importance of modeling these systems to ensure the economic viability of the system and the efficient planning layout is powerfully demonstrated. In this context, a typical research recently presented by Dahash et al. [24] paid more attention to discussing the PTES modeling parameters and models.

Despite the efforts by the authors mentioned above regarding introduction, construction, modeling method, and performance indicators, we detected there are still some deficiencies in the summary of PTES. Newly developed technical elements and modeling methods have not been updated. The technical challenges in practice have not been addressed properly. Furthermore, the different numerical approaches developed for PTES have not been thoroughly analyzed and compared.

Therefore, this work aims to provide a thorough update to help better understand the research and development of PTES. Compared with the previous review works, the innovations of this paper are:

- It covers all the technical aspects that affect PTES thermal performance, especially novel designs in recent years;
- It provides a list of thermal properties of various materials currently used on PTES, along with their strengths, weaknesses, and application status;
- It reviews systematically the numerical studies, focusing on the analysis of the mathematical theory concerning different methods;
- It discusses the application status of PTES and emphasizes the lessons learned from operational data across all projects.

This paper can be easily used by researchers and industry experts

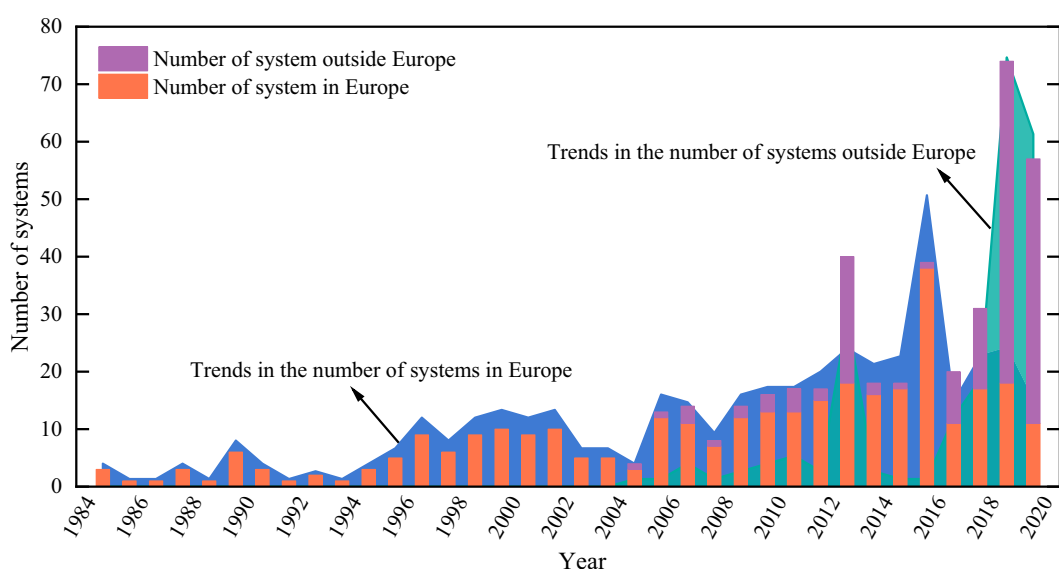


Fig. 1. Number of existing solar district heating systems worldwide during the last 35 years [3].

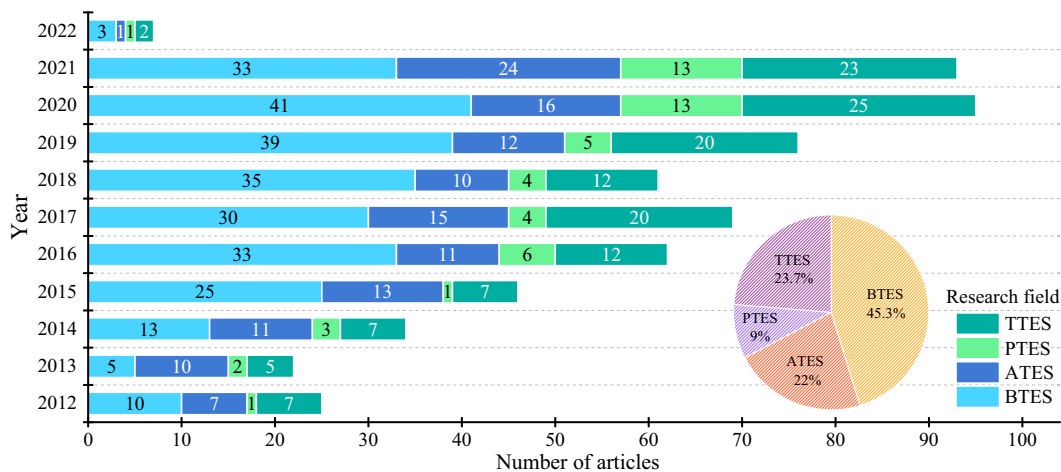


Fig. 2. Number of articles related to seasonal thermal energy storage from 2012 to 2022.

who need a quick and handy reference in PTES system design. Additionally, based on this review, readers may identify the existing research gaps in technical elements, numerical studies, and applications, which will aid them in proposing new research directions to fill the gaps.

The structure of this paper is illustrated in Fig. 3.

First, a summary of the key technical elements of PTES design is provided, including geometry, inlet/outlet diffusers, cover, insulation material, and liner material, highlighting PTES structure design challenges to understand possible further solutions and improvements. Recent research limitations are remarked by comparing recently used insulation and liner materials. The analysis of up-to-date numerical studies on PTES follows. They are categorized so the readers can understand the characteristics and applicability of various models. Additionally, models' calculation accuracy through experimental validation is compared, along with a detailed analysis of recent model assumptions and corrections with an aim to point out potential research directions.

Finally, the implemented PTES systems worldwide are summarized with particular attention to storage material, geological design, operation strategy, and storage duration. In order to learn lessons from actual operations, particular efforts are paid to collect and compare operational data on solar fraction, storage efficiency, and operation temperatures of PTES.

## 2. Technical elements of PTES

Due to the dispatchability and flexibility to incorporate various renewable energy systems, PTES is an essential part of solar district heating systems [25]. The thermal energy can be stored in an excavated ground enclosed with waterproof liners or can be stored in an artificial store composed of concrete or stainless steel for solar district heating systems with PTES [22,26].

The structure and the materials used on PTES are primarily the two

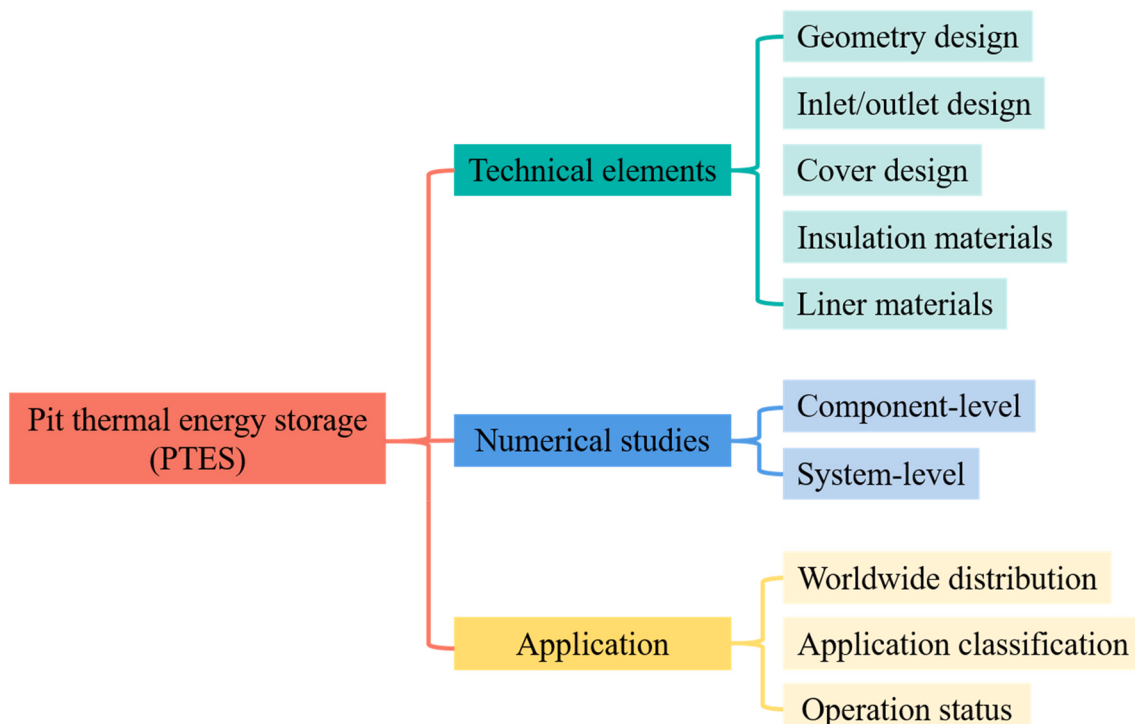


Fig. 3. Research work conducted for PTES technology.

factors that limit its development. Though conceptually comparable to TTES, PTES is more difficult to implement because of its structure and installation location. Given that the thermal performance depends on a wide range of interrelated factors, the design of a PTES is frequently considered sophisticated. Such factors are geometry, inlet/outlet design, and cover design. In addition, the materials used for PTES (i.e., insulation and liner) can severely affect the performance and the lifetime. In the following section, a thorough summary of the current technological status of the structure and materials, discussion and recommendations for future development are provided.

## 2.1. Structure of PTES

### 2.1.1. Geometry of PTES

Due to lower construction cost, storage geometries with slopes have been developed, such as pyramid stumps with rectangular cross-sections (Fig. 4 (a)) and truncated cones with circular cross-sections (Fig. 4 (b)). Geometry (a) is more commonly used due to conventional construction than geometry (b). Additionally, to satisfy the greater PTES volume requirements, a complex pyramid stump was created and used in the Vojens plant (see Fig. 4 (c)).

The slope angle is the angle between the sidewall and horizontal plane. It should be noticed in Table 1 that the slope angle is around 30° for PTES larger than 10,000 m<sup>3</sup> to prevent sidewall collapse [22,27–29]. In addition to the influence of the construction site's geological conditions on the slope angle determination, the selection of slope angle is also constrained by the thermal performance of PTES since the slope angle impacts the surface-to-volume ratio, which in turn affects heat loss [5,14,30]. A simulated analysis by Chang et al. [26] revealed that high slope angles were better for establishing and maintaining thermal stratification, and the heat loss could be reduced by increasing the slope angle. In this case, it seems reasonable to use the highest possible slope angle from the standpoint of reducing heat loss, improving thermal stratification, and reducing costs.

However, moving groundwater can enormously increase heat loss

from the lower parts of PTES. Therefore, future research is required to elucidate the ideal geometry for PTES installed in groundwater-moving sites.

### 2.1.2. The inlet and outlet design

Thermal stratification in solar stores significantly impacts the thermal performance of solar district heating systems, regardless of the type of system [59]. Investigations have shown that water supplied to hot water tanks can create mixing that spoils the thermal stratification in the storage tanks. As a result, all inlets and outlets must be designed to make the mixing as small as possible [60]. Compared with the widely used domestic hot water tanks, the size of thermal energy storage in solar district heating systems is larger. Diffuser design is typically adopted to reduce the velocity of water entering the thermal energy storage and encourage stratification by promoting laminar flow during charging and discharging processes.

Various structural characteristics may have an impact on the performance of the diffuser, and different diffusers may be useful for different thermal energy storage. Some diffuser designs, including H-type, octagonal, and radial diffusers, have successfully been investigated [61]. Shah and Furbo [59] investigated the impact of three inlet designs (i.e., pipe design, metro design, and plate design) on the thermal conditions inside the storage tank. Both simulation and experimental results proved that the plate type design had the highest degree of stratification. Chung et al. [62] studied the effect of design factors on the stratification of a rectangular storage tank by comparing three diffuser designs (i.e., the H-beam type, the radial plate type, and the radial adjusted plate type). Study results showed that the Reynolds number was the most critical parameter, and the radial plate type diffusers suppressed the local mixing more effectively than the H-beam type. Fagerlund Carlsson [63] compared the effect of different inlet designs and volume flows on mixing and found that the parallel plates were the best design that reduced mixing most, while the T-piece was the second-best design. The perforated and the direct pipe designs ranked third and fourth. Monchoco-Esteve et al. [64,65] studied the influence of different inlet constructions

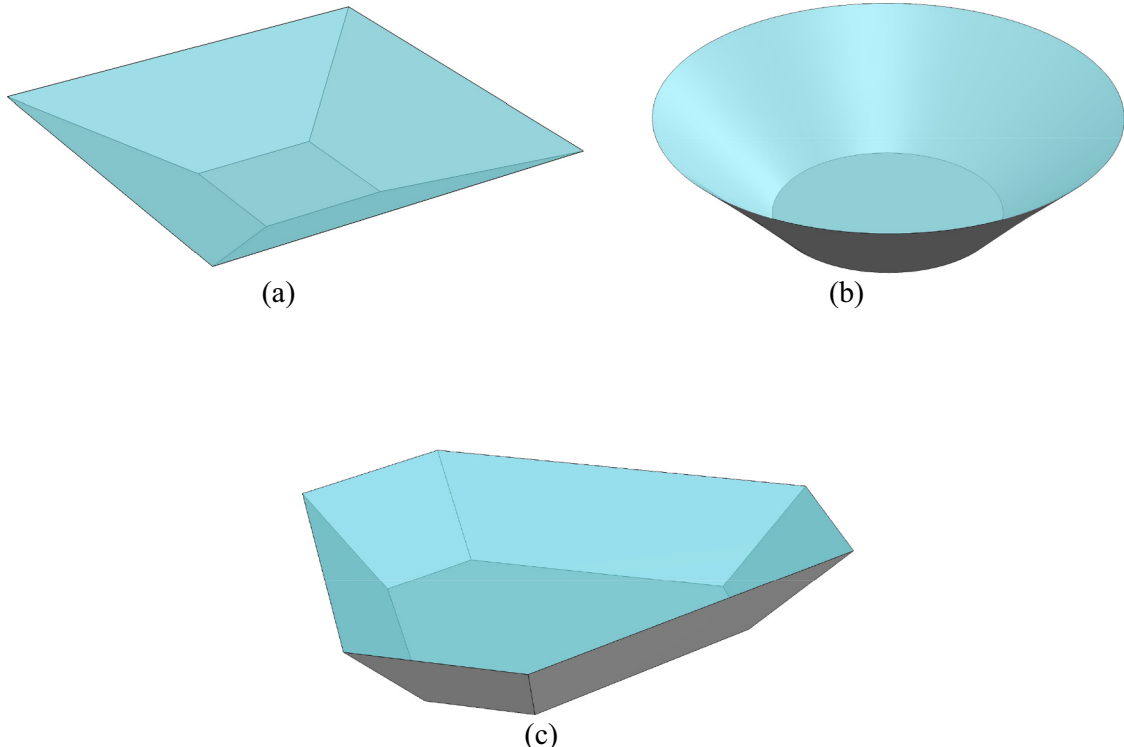


**Fig. 4.** Geometries of PTES: (a) truncated pyramid stump; (b) truncated cone; (c) complicated pyramid stump.

**Table 1**

Information on PTES of the existing plants.

Location	Heat store material	Volume (m <sup>3</sup> )	Area <sup>a</sup> (m <sup>2</sup> )	A/V <sup>b</sup>	Height (m)	Slope angle (°)	Inlet/outlet arrangement <sup>c</sup>	Liner material	Insulation material	References
Lambohov	Gravel & water	10,000	1750	—	—	90	—	Butyl Rubber	Clay granules	[30,31]
Stuttgart	Gravel & pebbles & water	1050	835	0.84	5	45	Heat exchanger from bottom to top	HDPE	Pumice and PUR	[32–34]
Julich	Water	2500	—	—	—	—	Horizontal heat exchanger in the bottom, the middle and the top	PP	Mineralwolle	[35]
Augsburg	Gravel & water	6500	—	—	—	90	—	—	—	[36,37]
Chemnitz	Gravel & water	8000	3375	0.43	6.76	90	Heat exchanger from bottom to top	HDPE	XPS	[30,31]
Steinfurt	Gravel & water	1500	1305	0.87	—	50	Heat exchanger from bottom to top	Foil PP Film	FGG EGG	[30,38]
Eggenstein	Gravel & sand	4500	1924.9	0.428	9	26 (top) 35 (bottom)	One is embedded in the bottom, the other in the top	HDPE	FGG Cellular particles	[27,39,40]
Marstal	Water	75,000	20,298	0.233	16	32.78	(b)	HDPE	Nomalen	[22,25,41–43]
Dronninglund	Water	60,000	17,076	0.288	16	26.6	(a)	HDPE	Leca	[28,41,44–47]
Gram	Water	122,000	28,893	0.237	15	20	(b)	HDPE		[4,48,49]
Vojens	Water	200,000	—	—	15	—	(b)	HDPE	Leca	[50–52]
Toftlund	Water	70,000	19,204	0.274	14.5	27	(b)	HDPE	Leca	[53–55]
Langkazi	Water	15,000	6748	0.447	—	27	(a)	HDPE		[56–58]
Tibet										

<sup>a</sup> Surface area of PTES (including the top surface, sidewalls, and bottom surface)<sup>b</sup> Ratio of PTES surface area to PTES volume.<sup>c</sup> The inlet and outlet arrangement of (a), (b) are shown in Fig. 6.

on thermal stratification in the storage tank. In their case, the sintered bronze conical diffuser performed better than other inlet constructions. Also, Assari [66] investigated the influence of the inlet and outlet location inside the storage tank on thermal stratification by simulation and experiment, respectively. He discovered that better thermal stratification occurred with an inlet of hot water in the highest position and cold water outflow from the lowest part. Findeisen et al. [67–70] conducted comprehensive studies to investigate the influence of radial diffusers on thermal stratification using CFD. They pointed out that thermal stratification could be significantly improved due to an optimized position of the diffuser in the storage tank. Besides, they proposed a new radial diffuser with a flow-optimized shape. Recently, Deng et al. [61] proposed a novel non-equal diameter radial diffuser and demonstrated that it had nearly the same thermal stratification performance as the equal diameter radial diffuser but significantly reduced the cost. Besides, the thermal stratification was optimized when the ratio of the long baffle diameter and the tank diameter was 1/3, the ratio of the short baffle diameter and the long baffle diameter was 1/3, and the distance between the two baffles was as small as possible.

In summary, radial diffuser design has been adopted in most existing PTES due to its simple structure, convenient installation, low cost, and good thermal stratification [61]. Radial diffuser design typically consists of two circular plates mounted parallel to each other (shown in Fig. 5 (a)), connected to the inlet/outlet pipe to form the water path. To help

produce uniform flow, guiding elements can be build-in (shown in Fig. 5 (b)). In real PTES application, diffusers are arranged at different heights at the top, the middle, and the bottom. Depending on the year-round operating conditions and PTES temperature distribution throughout the year, diffusers are either taken as inlet or outlet.

At present, there are generally two ways for the leading pipes to enter the PTES to connect the diffusers. One way is to enter through the bottom of the PTES (Fig. 6 (a) [71]), which is used in the Dronninglund and Langkazi plants. The other way is to enter through the side of the PTES (Fig. 6 (b) [25]), which is used in the Marstal, Vojens, and Toftlund plants. Compared to the design entering through the side, leading pipes entering the bottom perpendicular to the liner makes it easier to connect the concrete structure and flange under the liner [72]. However, the leading pipes have to be buried deeper in the ground, which may increase the thermal loss.

### 2.1.3. The cover

Most heat losses occur at the top of the PTES, based on the lessons learned from completed projects. Additionally, the cover accounts for most of the cost due to the complicated structure. For these reasons, much effort has been put into investigating different designs and materials [20,44,72–74]. There are now three main technical challenges.

One of the challenges is the insulation and liner material. Usually, the cover has three main layers (an insulation layer in the middle and

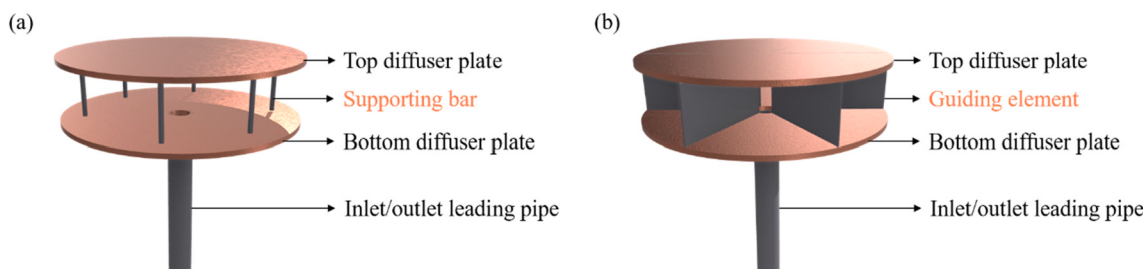


**Fig. 5.** Diffuser design: (a) diffuser design without guiding elements; (a) diffuser design with guiding elements.



**Fig. 6.** Arrangement of inlet/outlet of existing PTES application: (a) leading pipe enter PTES through the bottom [71]; (b) leading pipe enter PTES through the side [25].

two liner layers on both sides of the insulation). Fig. 7 (a) [10,25] shows the cover design of the Marstal and Dronninglund projects. Three layers of 80 mm Nomalén insulation were installed in the middle. One 1.5 mm and one 2 mm HDPE line, correspondingly, were put above and below

the insulation layers. Steel anchors were buried within the insulation layer to maintain the shape, and the hypernet CN-E layer was used to protect the liner. The cover design of Vojens and Gram projects is depicted in Fig. 7 (b) [75]. For two reasons, Leca was chosen as the

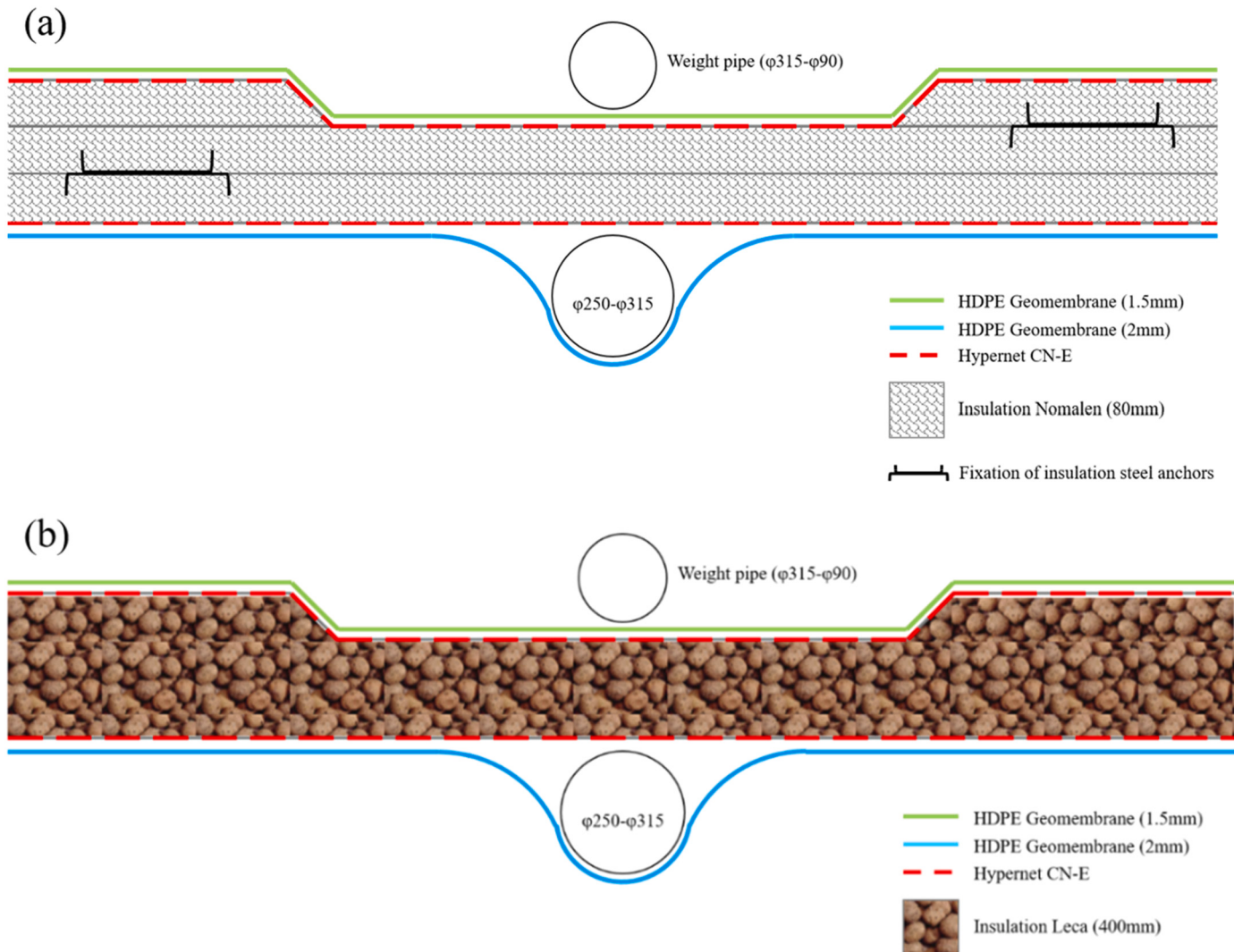


**Fig. 7.** Cross-section of the cover: (a) cross-section of the cover of Marstal and Dronninglund PTES [10,25]; (b) cross-section of the cover of Vojens and Gram PTES [75].

insulation material instead of Nomalén. One was that Leca was flexible and easy to install. The other was that Leca outperformed Nomalén in terms of thermal performance. However, there is no document to state the improvement clearly.

One of the challenges is to remove the moisture inside the cover. Moisture may result from the implementation phase of the cover, water diffusion through the liner, or damage to the liners. In this case, the insulation material will be degraded, resulting in increased thermal conductivity and reduced service life. Setting a ventilation gap (3–6 mm) between the liner and the insulation is a practical construction to remove moisture. At the same time, ventilation hoses are connected to the gap to help suck the moisture out in time.

The rainwater presents another challenge. Rainwater introduces a risk of puddles of water on the cover, which presses or even destroys the bulk insulation. Because of this, the cover is typically constructed with a 2 % slope towards the center of the cover. Additionally, the weight pipes made of HDPE with concrete inside will place on the top of the cover [76]. On the one hand, to help keep the liners in position in case of wind. On the other hand, direct rainwater collected on the top of the cover to the center pump. The weight pipe layout on the top of the cover of the

Marstal project is presented in Fig. 8 (a) [77]. The diameter of the pipe increases with distance from the center. In this manner, rainwater can be gathered in the center to lessen the possibility of water puddles on the cover [28]. Worth pointing out that additional effort should be paid when the geometric shape of the cover is changed. The arrangement and dimensions of the weight pipes need to be adjusted, as seen in Fig. 8 (b) [10].

Recently, Aalborg CSP created a new cover design in which the cover was divided into smaller sections (Fig. 9 (a) [78]), each with an individual drop towards the center pump (Fig. 9 (b) [79]). This makes it considerably simpler to direct rainwater away from the surface and makes it possible to build larger PTES [78]. Additionally, the fall on the under and upper sides of each section shown in Fig. 9 (b) [79] ensures that the air pockets are discharged [79]. Moreover, a diffusion-open structure is another innovation of the new design, preventing vapor accumulation inside the insulation layer. The functional performance of the new design has been inspected and verified, but no data exist to demonstrate the improvement effect.

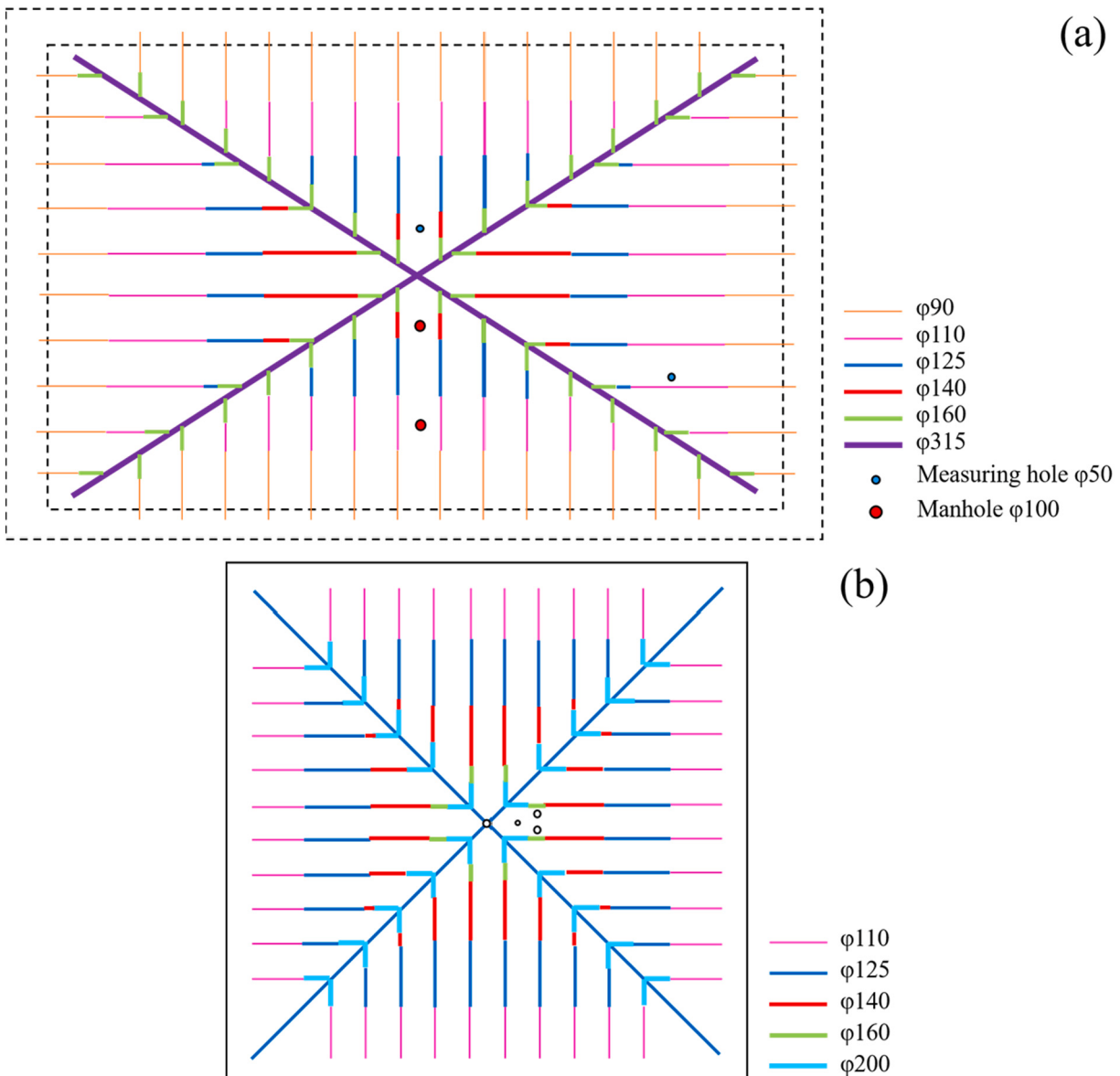
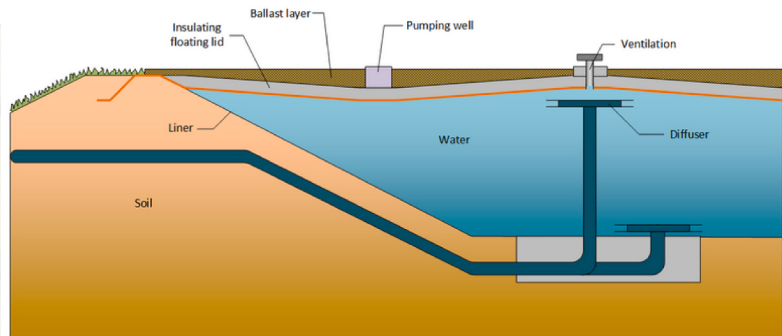


Fig. 8. Weight pipe layout on the top of the cover: (a) weight pipe layout of Marstal plant [77]; (b) weight pipe layout of Dronninglund plant [10].



(a) Top view



(b) Principle sketch

**Fig. 9.** New cover solution developed by Aalborg CSP [78,79].

## 2.2. The materials used for PTES

### 2.2.1. Insulation materials

Most of the heat loss in uninsulated PTES is lost through the cover and upper edges [80]. As a result, a thicker layer of insulation will be

added inside the cover, as previously mentioned. The side and bottom walls of PTES are rarely insulated because the surrounding soil can act as a heat reservoir and transfer heat back to the PTES during discharge. However, insulation of the bottom wall is still recommended when it is closed to groundwater [81].

**Table 2**  
Properties for insulation materials.

Material	Grain size (mm)	Thermal conductivity (W/(m·K) <sup>a</sup> )	Density (kg/m <sup>3</sup> )	Moisture effect on thermal conductivity	Advantages	Disadvantages	References
EGG	2–4	0.07 <sup>b</sup> 0.08 <sup>c</sup>	200 <sup>b</sup> 190 <sup>c</sup>	5 times (T = 60 °C; M = 200 kg/m <sup>3</sup> ) <sup>e</sup>	Easy to install Cost-effective	High cost	[25,81,82,86]
	4–8	0.08 <sup>b</sup>	185 <sup>b</sup>	10times	High temperature resistance		
	8–16	0.08 <sup>b</sup>	140 <sup>b</sup>	(T = 60 °C; M = 200 kg/m <sup>3</sup> )	Lightness	Low moisture resistance	[20,44,81,82,87]
	1–4	0.08 <sup>c</sup>	300 <sup>c</sup>	–	High strength	Lack of demonstrated in reality	
ECG	4–8	0.1 <sup>b</sup>	270 <sup>b</sup>		High drainage capacity		
	0–20	0.06 <sup>b</sup>	150 <sup>b</sup>	–	Lightness		[81,88,89]
GFG	10–50	0.09 <sup>c</sup> 0.08 <sup>d</sup>	195 <sup>c</sup> 170 <sup>d</sup>	–	Dimensionally stable Lightness		[81,82]
PUR/PIR foam	–	0.02–0.03	80	Increase from 0.025 W/m K to 0.046 W/m K with increasing moisture content from 0 vol% to 10 vol%.	High temperature resistance High moisture resistance	High temperature expansion	[25,37,89,90]
Nomalén28N	–	–	28	–	High heat resistant High-temperature resistance High moisture resistance		[44,91]
Mineral wool	–	0.03–0.04	160	Increase from 0.037 W/m K to 0.055 W/m K with increasing moisture content from 0 vol% to 10 vol%.		Low moisture resistance Hard to dry out	[20,89,90,92]
EPS	–	0.03–0.04	15–40	Increase from 0.036 W/m K to 0.054 W/m K with increasing moisture content from 0 vol% to 10 vol%.	Low thermal conductivity High water resistance	Stiff Become fragile after absorbing water	[20,90,93]
Perlite	0–1	0.05 <sup>b</sup>	90 <sup>b</sup>	–	Suitable for high temperature	Light-weight Difficult to control during implementation Difficult to make solid enough for treading on	[81,84]
Mussel shells	–	0.11–0.15	1070	–		Heavier than water; Higher thermal conductivity Difficult to be self-sustaining	[20,25,94]
Poraver	–	–	–	–	–	High material cost	[20]

<sup>a</sup> The thermal conductivity is under manufacturer specification.

<sup>b</sup> Type I.

<sup>c</sup> Type II.

<sup>d</sup> Type III.

<sup>e</sup> Moisture content at temperature 60 °C.

In the earlier stages of PTES design, the choice of insulation material is a crucial step that ultimately impacts PTES performance. The following desired specifications for insulation materials are generally agreed-upon: high thermal conductivity, high moisture resistance, high-temperature resistance, low density, low cost, and easy to install. There is, however, no perfect insulation material that satisfies all the requirements, and each material has its advantages and disadvantages. A list of tested insulation materials that met manufacturer requirements is shown in Table 2. Additionally, their thermal properties under specific experimental conditions, as well as strengths and weaknesses based on practical application, are included.

Together with Table 1, it can be observed that in earlier projects, sheets of rock wool, mineral wool, or polystyrene (expanded polystyrene (EPS) or extruded polystyrene (XPS)) were installed on the walls and the cover. But mineral wool and EPS will become too vulnerable if water infiltrates the insulation [81]. In this context, it is replaced by bulk insulation like expanded clay granules (EGG) or foam glass gravel (FGG). Bulk insulation also has the benefit of requiring less installation time and cost, particularly for large-scale PTES, since it can be installed by blowing from a silo truck [27,82]. Nomalén and Leca have lately been suggested to be more suited for insulation usage due to their superior thermal performance.

As far as we can obtain in the literature, the majority of insulating materials have their thermal properties tested under typical application conditions, and it is yet uncertain how thermal properties change under high temperature and high humidity conditions. Limited literature has

revealed that, especially at higher temperatures, the thermal conductivity of the insulation increases dramatically with increasing moisture content [82,83]. Consequently, it has been found that the yearly thermal losses of most solar district heating plants with buried PTES are around 30–50 % or even considerably greater than the design values [30,81,82,84,85].

## 2.2.2. Liner materials

The liner encloses the water body on both sides of the cover to protect the insulation materials so that it has a significant role in determining the lifetime of a PTES. Moreover, by preventing vapor from traveling through insulation, the liner can help reduce heat loss [24]. The most common liners used for PTES are made of stainless steel, polymers, and elastomers [24,30,44]. Stainless steel was used as the liner in early plants (as shown in Table 1), but it was replaced by polymeric liners due to lower material costs and installation costs, especially for storage volumes larger than 20,000 m<sup>3</sup> [95,96]. However, offers for pilot storage in Rottweil had pointed out that a stainless steel liner with 0.5 mm thickness could be installed for roughly the exact cost as a thicker PP liner. In this context, a novel approach for assessing the liner material should be developed to consider many objectives. Otherwise, thicker polymer liners could be more expensive than thinner stainless steel with the same water resistance.

The thermal properties of liner material used to date are listed in Table 3. All listed polymer liners realized high water vapor permeability except for high-temperature polymer liners (HDPE). As a result, the

**Table 3**  
Properties for liner materials.

Category	Material	Thermal conductivity (W/(m K) (at °C)	Water vapor permeability (g/m <sup>2</sup> /day)	Lifetime (years) <sup>a</sup>	Advantages	Disadvantages	References
Polymer liners	HDPE	0.44 (25 °C)	0.03 ( $\sigma^b = 1 \text{ mm}$ , $T^c = 20 \text{ }^\circ\text{C}$ ) 1.5 ( $\sigma = 2.5 \text{ mm}$ , $T = 80 \text{ }^\circ\text{C}$ )	<3 ( $T = 90 \text{ }^\circ\text{C}$ ) 24.3 ( $T < 70 \text{ }^\circ\text{C}$ ) 1.45 ( $T = 100 \text{ }^\circ\text{C}$ ) 0.92 ( $T = 107 \text{ }^\circ\text{C}$ ) 180 days (115 °C) >20 ( $T = 90 \text{ }^\circ\text{C}$ ) <sup>d</sup>	Low material cost Easy to install Low installation cost	Complicated temperature resistance Poor water vapor permeability	[20,30,44,72,74,98–100]
	PP	0.11 (25 °C)	4 times as high as for HDPE	<6 ( $T = 80 \text{ }^\circ\text{C}$ ) 22.6 ( $T < 70 \text{ }^\circ\text{C}$ ) 1.1 ( $T = 100 \text{ }^\circ\text{C}$ ) 0.55 ( $T = 107 \text{ }^\circ\text{C}$ ) 0.33 ( $T = 115 \text{ }^\circ\text{C}$ ) 16 ( $T = 85 \text{ }^\circ\text{C}$ )	Less degradation in contact with water Low material cost Easy to install Low installation cost		[20,44,72,95]
	PE	0.4 (23 °C)	–	15 ( $\sigma = 2 \text{ mm}$ , $T = 95 \text{ }^\circ\text{C}$ ) 18 ( $\sigma = 3 \text{ mm}$ , $T = 95 \text{ }^\circ\text{C}$ ) 1 ( $T = 85 \text{ }^\circ\text{C}$ )	Low material cost Easy to install Low installation cost		[20,44,95,101]
	LDPE	0.33 (23 °C)	45 times as high as for HDPE	–			[44,102]
	PVC	0.14–0.17 (25 °C)	115 times as high as for HDPE	–			[44,103]
Elastomer liners	EPDM	0.29 (25 °C)	2 times as high as for HDPE	–	Low material cost Higher temperature resistance	Not weldable Need special glue Higher installation cost	[44,72,104,105]
Metal liners	SST AL <sup>e</sup>	25 (20 °C) 239 (20 °C)	–	–	Long term stability Higher vapor tightness Highest temperature resistance	High material cost High installation cost Need special welding equipment	[44,72,106,107] [44,72,107]

<sup>a</sup> Most of the results were tested by the Danish Technological Institute or assessed using a micro specimen.

<sup>b</sup> Thickness of liner.

<sup>c</sup> Experimental temperature.

<sup>d</sup> It is offered by the supplier, but has not been tested yet.

<sup>e</sup> Aluminum is not appropriate because of the pH in the storage water.

demand for HDPE liners has accelerated [30]. However, the water vapor permeability of polymer liners is strongly independent of temperature [97], which can be seen from the change in water vapor permeability of HDPE at different temperatures. When HDPE is tested at 1 mm thickness under 20 °C, the water vapor permeability is 0.03 g/m<sup>2</sup>/day, while when HDPE is tested at 2.5 mm thickness under 80 °C, the water vapor permeability can reach 1.5 g/m<sup>2</sup>/day.

Considering the service life of liner materials, only three of them can be found in the literature, and most of the data are supplied by the Danish Technological Institute. Compared to the applications of such materials for hot water piping, the maximum service temperature and the exposure times are significantly higher for PTES. Therefore, reliable information on the service life of liners used for PTES under higher temperatures, especially under actual operation conditions, needs future investigations [30,72]. A newly developed high-temperature HDPE liner that can last >20 years at 90 °C was claimed and guaranteed by the supplier recently. Still, it was not yet tested according to reliable methods [15].

### 2.3. Summary and outlook of PTES technical elements

The technical elements will determine the investment costs of PTES and, more importantly, will significantly affect the storage efficiency over its lifetime [84]. The optimal design of PTES still face several difficulties.

#### 2.3.1. Structure of PTES

At present, the geometry of PTES of most projects is regular, but due to the influence of geological conditions, more and more irregular-shaped PTES may appear. In this context, it is vital to understand the impact of geometry changes on PTES thermal and economic performance. Moreover, providing bottom insulation depends on many aspects, such as operation conditions, PTES bottom temperature, and soil parameters. These factors should be considered in the cost-benefit analysis of different insulation designs.

Investigations into the diffuser design have been conducted numerically and experimentally. The majority of studies, however, have focused on small-scale thermal energy storage. The structure of large-scale PTES with diffusers has not received much attention since it is time-consuming. The results from small-scale investigations must be carefully considered when scaling up because the PTES has a much bigger volume than a heat storage tank. What is more, the effect of inlet/outlet position or operating parameters on the performance of PTES has been partially understood, making engineers rely heavily on experience. Consequently, it is necessary to perform a full-scale simulation of PTES to identify the optimal inlet/outlet designs under different conditions.

As a crucial part of PTES, proper configuration and installation of the

cover with insulation layers are challenging since thermal insulation and vapor permeability must be considered simultaneously. To prevent damage to the insulation, the amount of moisture entering the insulation layer is reduced as much as possible. Additionally, more attention should be paid to thermal bridges caused by connection parts.

#### 2.3.2. The material used for PTES

The envelope of the buried PTES has to fulfill numerous vital purposes. As a summary and comparison of the aforementioned materials, Fig. 10 and Fig. 11 plot thermal conductivity against density for insulation materials and thermal conductivity against test temperature for liner materials, respectively. Clearly, these are fewer materials available for PTES at the moment.

As demonstrated in Fig. 10, except for mussel shells, the thermal conductivities of insulation materials range from 0.01 W/(m·K) to nearly 0.1 W/(m·K) and densities are lower than 300 kg/m<sup>3</sup>. Changes in thermal conductivities are recorded for only four materials whose moisture changed. It is worth noting that the thermal conductivity change after water absorption by EGG appears to be unacceptably high. The applicability of other materials is still uncertain because no additional information is available.

No waterproofing membranes developed especially for buried PTES, so liner materials used in other areas must be used. However, materials used in other fields often do not meet the high demands of temperature resistance. Currently, recorded thermal conductivity is limited to the range of 20 °C to 30 °C. The thermal conductivity of all other materials, excluding metal liners, is <0.6 W/(m·K). In addition, only the lifetime of three materials at different test temperatures can be collected, as shown in Fig. 11. The service life of HDPE and PP liners appears to decrease with rising temperatures, but research findings are inconsistent, which may be due to differences in experimental parameters and methods. To elucidate the details, it is necessary to comprehend the aging mechanisms of liner materials, and particular focus must be placed on the investigation of polymeric accounting for the more severe temperature load profiles [101].

In conclusion, in order to reduce heat losses, new insulation materials with low thermal conductivity need to be developed. It is also desirable to compare various thermal insulation materials in terms of thermal conductivity, durability, water resistance, as well as installation costs [92]. Future research should focus on novel liner materials (e.g., bentonite, bitumen, geo-membranes, and high-performance concrete [24]), especially its long-term durability for temperatures higher than 90 °C. One aspect that needs special consideration is that the liner material research should take into account both the temperature and pH of water in the PTES.

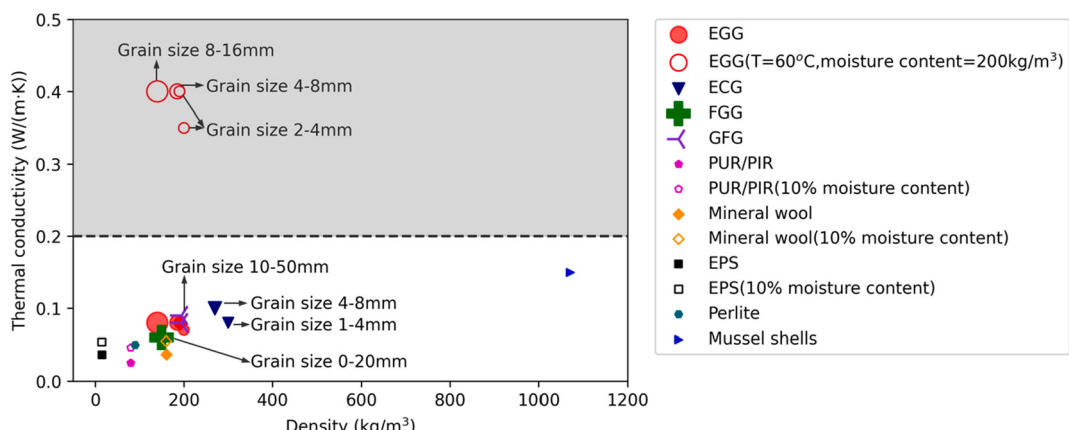


**Fig. 10.** Thermal properties of insulation materials mentioned in the literature [81,82,84,88–90,92,94].

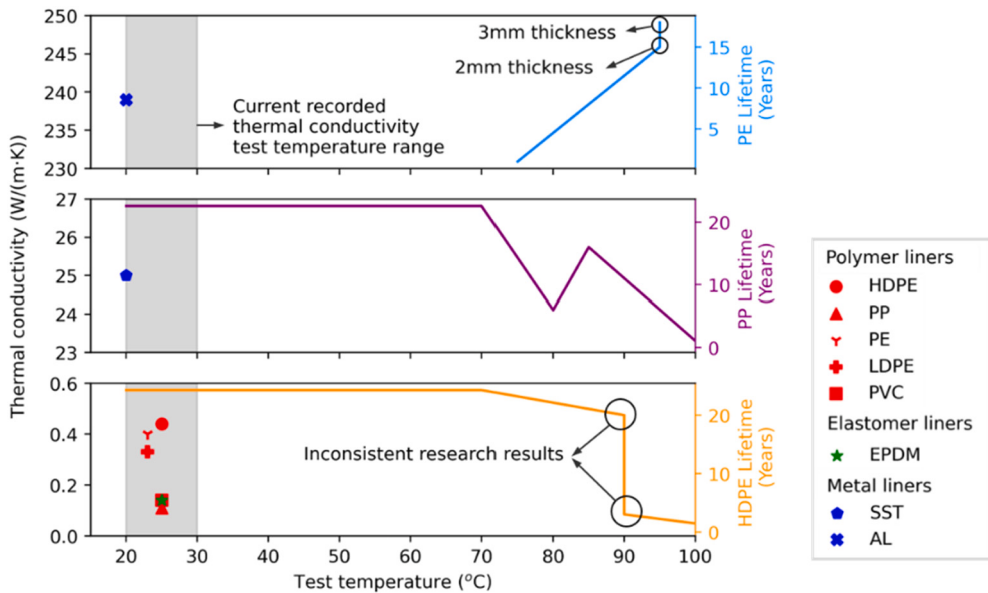


**Fig. 11.** Thermal properties and lifetime of liner materials mentioned in the literature [44,72,74,95,99,102,103,105,107].

### 3. Numerical study of solar district heating plants with PTES

Proper planning is critical to commission the STES and assure the projects' economic viability [108]. As a result, the simulation methods for STES have received much attention [109], whereas most numerical research concentrates on TTES, BTES, and ATES because these three storage types are widely used in practice and have more mature simulation models. In contrast, PTES is a relatively new technology with limited available monitoring data, and modeling PTES is challenging due to complicated geometries. So far, only a few publications on PTES modeling studies can be found (see Table 4). The main findings and drawbacks of those studies are also added to Table 4 to provide a preliminary understanding.

Recent numerical studies can be clarified into component-level (i.e., considering only the performance of PTES) and system-level (i.e., integrating PTES into solar district heating systems). This section of the review presents all the available numerical models, with special attention to the mathematical theory and their calculation accuracy.

#### 3.1. Numerical study of PTES

Over the years, several models have been created to allow quick and trustworthy calculation of PTES performance. The energy balance equation is typically solved in such models using three approaches, the finite difference method, the finite element method, and the finite volume method. Based on these three approaches, this part discusses the numerical study on the component level in depth.

##### 3.1.1. Approaches based on finite difference method

For the finite difference method, the water and soil regions are typically divided into nodes. The calculation algorithms consider the mass and energy flow, conduction between different nodes, and heat transfer through the walls. The commonly used finite difference method is implemented as TRNSYS models, including Type 342, Type 343, Type UGSTS, Type 1300-1301, and Type 1322. Fig. 12 [110–112,115,116,127] displays the geometric and grid characteristics of different models, as the grid division method determines the complexity of the model and impacts the model's calculation accuracy.

In terms of storage region (i.e., PTES marked in Fig. 12 [110–112,115,116,127]), all of these models are simplified to one dimension. The storage region of Type 342 and Type UGSTS are

restricted to cylinder geometry, while Type 343 and Type 1300-1301 extend the geometry to axisymmetric cones. The newly developed Type 1322 from TESS can also be used for symmetrical square pyramids. Besides, the storage region can be divided equally and unequally in height in all these models, which needs careful consideration when modeling, as calculation accuracy may be significantly affected.

For soil region, Type 1322 is three dimensions and other models are two dimensions. It is evident from Fig. 12 [110–112,115,116,127] that the mesh division of the soil region varies significantly between models. For Type UGSTS, Type 343 and Type 1300-1301, the mesh density for part 1st and 2st in the z direction are determined by the nodes number in the PTES. However, the mesh density of part 2st for Type 342 can be set independently, with a factor towards the top and bottom contours of the storage region. Common to all models is that denser grid is applied in the adjacent area to more accurately calculate heat transfer between the storage and soil. Notably, there is an encryption above and below the baseline of the storage grid division interface for Type 1300-1301, designed to accurately simulate the thermal stratification intersection where temperature jump exists.

Several studies have been devoted to evaluating PTES performance using these finite different models. Raab et al. [127] validated Type 342 with the Hannover solar-assisted district system. Simulation results showed that the calculated temperature agreed well with the measured temperature, yet the heat loss through the bottom wall was severely overestimated. Pan et al. [110] also studied the performance of PTES using Type 342, with certain modifications made to fit the operation characteristics of the Dronninglund plant. The modified model predicted well the storage temperatures and the heat flow. For one year validation, the deviations of annual charged/discharged energy, internal energy content, and annual thermal loss between the model and the measurement were 2.0 %, 1.9 %, 2.5 %, and 1.1 %, respectively.

Xie et al. [112] developed a PTES model for the Dronninglund plant based on Type 343. Their numerical findings demonstrated that the accuracy of the modified model was acceptable, and soil properties had an important influence on storage efficiency. However, the calculated deviation of PTES and soil temperature near the ground level could reach 16 K and 4 K, respectively.

Bai et al. [115,116] developed Type UGSTS and validated it with experimental data of an actual project in Huangdicheng, China. The results showed that the model could accurately predict the temperature trend in the water and soil. At different heights from the PTES bottom,

**Table 4**

Conclusion of the reference publications on PTES.

Authors	Year of publication	Simulation approach/tool	Model dimension of PTES	Creativity and main findings	Drawbacks
Pan X. et al. [110]	2022	PTES/TRNSYS	1D model (water part) 2D model (soil part)	(1) Validated a modified Type 342 with measurement data; (2) Storage cycle has a significant impact on storage efficiency;	(1) Limited to cylinder structure; (2) Large monthly differences heat loss between simulation and measurement;
Gauthier [111]	2020	PTES/TRNSYS	1D model (water part) 2D/3D model (soil part)	(1) Propose new model (Type 1300 + 1301 and Type 1302); (2) Type 1300 + 1301 and Type 1322 gave better results than Type 342; (3) Type 1300 + 1301 cost less calculation time;	(1) Limited to symmetrical structure; (2) Limited ports for Type 1300 + 1301 and Type 1302; (3) Large predicted side and bottom heat loss error for Type 342
Xie Z. et al. [112]	2020	PTES/TRNSYS	1D model (water part) 2D model (soil part)	(3) Validated a modified Type 343 with measurement data; (4) Considerable heat extracted from the soil in winter; (5) The middle diffuser height affect the storage efficiency;	(1) Limited to symmetrical structure; (2) Large monthly differences heat loss between simulation and measurement;
Narula K. [113]	2020	System/Mathematical model	1D model (water part) 2D model (soil part)	(1) Validation with Marstal monitored data; (2) Preliminary assessment of the DH system without using specialized software;	(1) Cannot replace detail simulation tools; (2) Large monthly differences between simulation and reported;
Kubinski K. et al. [114]	2020	System/Aspen Hysys	1D model (water part)	(1) Model development on Aspen Hysys	(1) Limited to cylinder structure;
Bai Y. et al. [115]	2020	PTES/TRNSYS	1D model (water part) 2D model (soil part)	(2) Trnsys is recommended for system simulation (1) Model development on Trnsys; (2) Validated with measurement data; (3) The PTES annual storage efficiency increases with sidewall slope; (4) Steeper slope gives better thermal stratification than smaller slope;	(2) Great simulation deviation; (1) Limited to symmetrical structure; (2) Limited to circular cross-section geometries; (3) Limited to two inlet/outlet diffusers;
Bai Y. et al. [116]	2020	PTES/Mathematical model	1D model (water part) 2D model (soil part)	(1) Insulation on the side of PTES is also important; (2) Compared to MIX number, the stratification number is more representative;	(1) Limited to symmetrical structure; (2) Limited to circular cross-section geometries;
Dahash A. et al. [117]	2020	PTES/COMSOL	2D model (water part) 3D model (soil part)	(1) Validated with data from Dronninglund project; (2) Potential of improving the stratification by shifting from sloped-wall thermal energy storage;	(3) Limited to two inlet/outlet diffusers; (1) Limited to symmetrical structure; (2) Limited to circular cross-section geometries;
Dahash A. et al. [118]	2019	PTES/COMSOL	2D model (water part) 3D model (soil part)	(1) Potential of improving the stratification by shifting from sloped-wall thermal energy storage; (2) Similar efficiency appears when tank without insulation and Pit with insulation after the ground pre-heating period;	Limited to the groundwater in the upper soil region;
Li X. et al. [119]	2019	System/TRNSYS	1D model (water part) 2D model (soil part)	(1) Control strategies; (2) The stratification of the seasonal storage; (3) Variable flow control is superior to temperature different control;	(1) Limited to circular cross-section geometries; (2) Groundwater is not considered; (3) Limited to two inlet/outlet diffusers;
Nageler P. et al. [120]	2019	System/IDA + DYMOLA DHS + TRNSYS	1D model (water part) 2D model (soil part)	(1) Propose a co-simulation framework; (2) Climate is important for system selection;	(1) The co-simulation framework is not validated;
Dahash A. et al. [121]	2018	PTES/COMSOL	1D model (water part) 2D model (soil part)	(1) Provide analysis for underground axisymmetric structures; (2) Model optimized with the respect to heat loss; (3) Low computation efforts;	(1) Limited to axial symmetric geometries; (2) Charging and discharging scenarios are simplified;
Sorknæs P. [109]	2018	System/Excel	1D model (water part)	(1) Validated with data from Dronninglund project;	(1) The system model only consists of the heat loss from the water pit storage and the heat pump itself; (2) Did not specify the errors between simulation and measurement results; (1) Small scale simulation; (2) Short-term simulation; (3) Inlet and outlet are not considered;
Chang C. et al. [26,29,122]	2017	PTES/FLUENT	3D model (water part) 3D model (soil part)	(1) Downward flow appeared next to the sidewalls; (2) Steeper slope gives significant temperature stratification; (3) Intense heat transfer process appears at the beginning of cooling; (4) Average Nusselt numbers on the inner surface of the sidewalls and the bottom are higher than that of the top thermal insulation layer;	(1) Short-term simulation;
Fan J. et al. [123]	2017	PTES/FLUENT	3D model (water part) 2D model (soil part)	Thermal stratification strongly depend on the temperature of water returned to the PTES;	(1) Demand more calculation time; (2) Short period simulation;

(continued on next page)

**Table 4 (continued)**

Authors	Year of publication	Simulation approach/tool	Model dimension of PTES	Creativity and main findings	Drawbacks
Chatzidiakos A. [124]	2016	PTES/FLUENT	3D model (water part) 2D model (soil part)	(1) Thermal stratification can be maintained in most cases; (2) Backflow and mixing can be avoided by a pieced vertical disc at the end of the large pipe or a suitable nozzle;	(1) Groundwater is not considered; (2) Ground temperature fluctuation with time is not considered; (3) Demand more calculation time;
Reiter P. et al. [125]	2016	System/TRNSYS	1D model (water part) 2D model (soil part)	(1) Heat price is competitive compared to heat from gas boilers for Graz; (2) Price stays in the economic sound range while solar district heating system size varying between 150,000 m <sup>2</sup> and 650,000 m <sup>2</sup> ;	Lack of depth investigation
Ochs F. [126]	2014	PTES/ Matlab+Simulink	2D model (water part) 2D model (soil part)	(1) Dynamic simulation; (2) Consider the variable distribution of the thermal insulation;	(1) limited to axial symmetric geometries; (2) Heat loss is not comparable to the measured data;
Raab S. et al. [127]	2005	PTES/TRNSYS	1D model (water part) 3D model (soil part)	(1) Modeling one volume segment at the storage bottom is important; (2) Temperatures in the ground and the heat losses through the bottom are significantly overestimated without bottom segment model;	(1) Limited to geometries with vertical sides. (2) Limited to axial symmetric geometries;

the average relative error of PTES temperature was around 2.5 %. However, the maximum deviation in calculated soil temperature could reach 5 K. Furthermore, by examining the influence of height and sidewall slope on the thermal performance of PTES, they pointed out that there existed an optimum height to minimize the annual heat loss of PTES.

To assess the applicability of various models in the calculation accuracy and time efficiency, Gauthier [111] calibrated three models (i.e., Type 342, Type 1300-1301, Type 1322) with measurement data from the Dronninglund plant. Calibration analyses with variable parameters proved that Type 1300-1301 and Type 1322 gave superior results to Type 342, especially for heat losses through the cover. Under the conditions of this study, the relative error of Type 342 for bottom and side heat loss prediction could reach 87 %. Moreover, Type 1300-1301 cost less calculation time than Type 1322, which was recommended for predicting the performance of PTES. Type 1322 could be used for detailed studies because of the sophisticated modeling theory. However, the heat loss from the bottom and sidewall of PTES could not be calculated accurately for all these models. Furthermore, more ports should be added to simplify the input file for Type 1300-1301 and Type 1322.

In addition to the models implemented in TRNSYS, Ochs [126] developed a dynamic model using the Matlab/Simulink platform that incorporated a one-dimensional finite-difference storage model and a two-dimensional finite element soil model. This model was adjusted to various symmetrical shapes. Fig. 13 [126] indicates the difference between modeling TTES and PTES due to the surroundings based on the simulation results. It can be seen that the TTES was less affected by its surroundings because of the insulation on its side and bottom walls, while PTES was greatly affected by its surroundings since its lack of insulation. Therefore, the performance of insulation materials should be the main consideration for TTES, and the heat transfer between the water and soil region should be the primary concern for PTES.

### 3.1.2. Approaches based on finite element method

Commonly, the finite difference method is used for structure geometry since it is easier to implement than the finite element and finite volume method when the computational region can be divided into structure grids [128]. However, newly constructed PTES varies from symmetric pyramid stump to asymmetric pyramid stump because of local geological properties and construction investment, posing significant challenges to the finite difference method.

At this level, Dahash et al. [24,117,118,121,129] developed a new model for symmetric PTES shapes with surrounding soil region using

COMSOL Multiphysics (Fig. 14 (a) [121]) based on their previous investigation. They observed that PTES performance would drop under realistic conditions because of the existing groundwater. Accordingly, a new model considering groundwater (Fig. 14 (b) [24]) was proposed and validated. Compared to the Dronninglund PTES measurements, the annual charge energy, discharge energy, internal energy, and heat loss deviate by <0.5 %, indicating the new model's reliability. Yet, some slight discrepancies were seen due to uncertainties such as the cover's overall heat transfer coefficient and the soil region's thermal conductivity. Especially during November and December, the maximum deviations of charging energy were >5 %.

Moreover, the influence of STES geometry on thermal stratification was demonstrated by comparing the MIX number between Dronninglund PTES and a corresponding cylindrical TTES. For the cylindrical TTES, better stratification and lower thermal losses were observed, making it essential to find a compromise between technical performance and economic viability.

### 3.1.3. Approaches based on finite volume method

Although approaches based on finite difference and finite element methods can be used to predict the performance of the PTES, they are not appropriate for detailed studies. The uncertainty in the boundary conditions will strongly impact the simulation results because they depend on numerous assumptions. As a result, some researchers used the finite volume-based ANSYS FLUENT to conduct in-depth investigations.

Chatzidiakos and Fan [123,124] built a real-scale PTES model in ANSYS FLUENT (Fig. 15 (a) [124]). Simulation results were presented for different typical cases (Fig. 15 (b) [123]) and showed that the simulated model predicted PTES temperatures satisfactorily within a 10 % difference for all these cases. Moreover, it proved that the mixing region was very limited in periods with slight temperature differences between inlet water and water inside PTES (Discharge case on October 7). But significant mixing occurred when the temperature differences were more considerable (Discharge case on February 18). Accordingly, powerful mixing would destroy thermal stratification and eventually affect the performance of PTES. The authors recommended paying more attention to investigating the position of inlet diffusers, the influence effect of inlet velocity, and the temperature difference between inlet water and water inside PTES.

Chang et al. [26,29,122] set up both experimental and simulation models of small-scale PTES. Natural convection along the sidewalls inside the PTES was investigated. The experiment proved that the simulation of the temperature curve was reasonable, and the maximum relative error was ±9.77 %. Additionally, simulation results illustrated

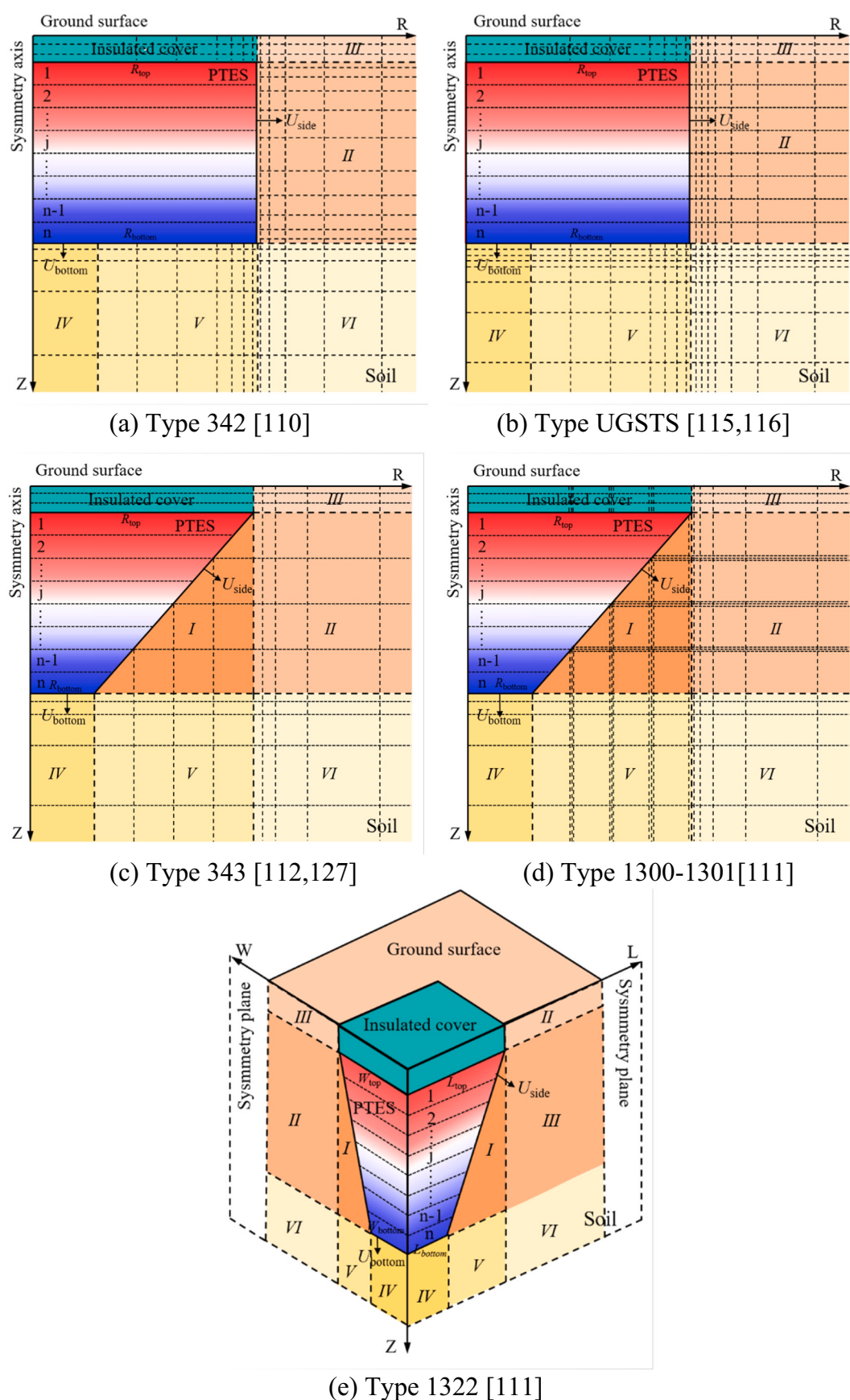
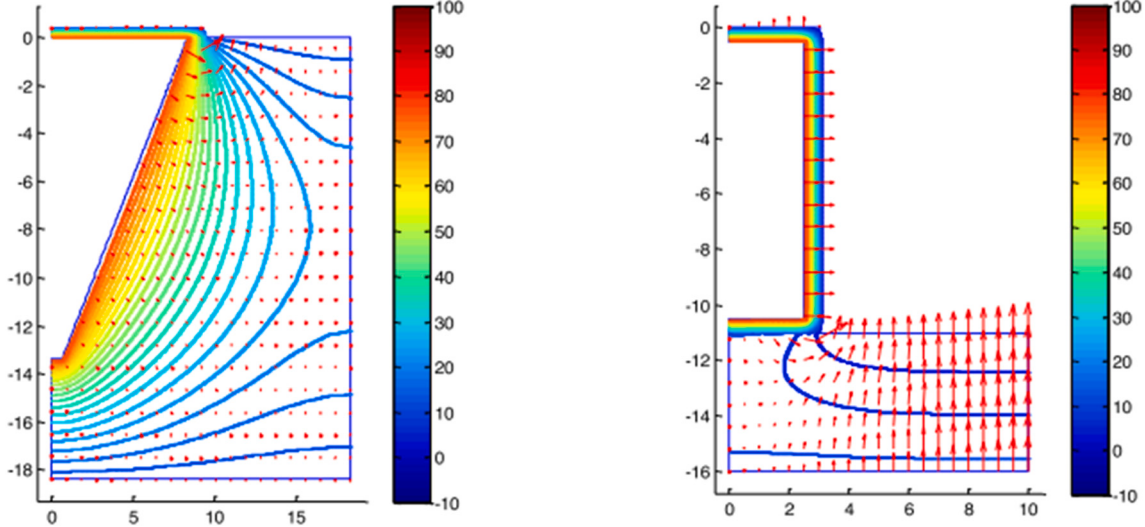
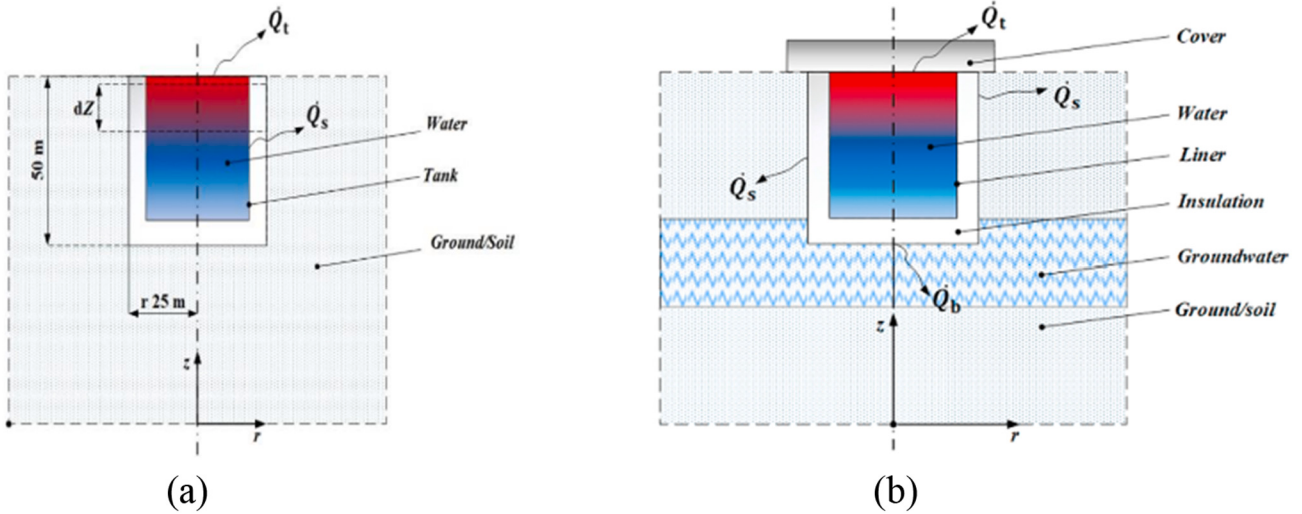


Fig. 12. Geometric characteristic and mesh method of models based on finite difference method.



**Fig. 13.** Temperature profile in the surrounding ground of a PTES (left) and TTES (right) with ground coupling [126].



**Fig. 14.** Schematic of an underground tank with its surroundings: (a) without groundwater [121]; (b) with groundwater [24].

that both the sidewalls and the surrounding heat loss affected the natural convection inside the PTES, which might create downward flow along the sidewalls (Fig. 16 [122]). It was worth noting that natural convection was more intense at the beginning of the cooling process. Furthermore, the influence of geometry on the thermal performance of PTES was studied. It concluded that a smaller depth and a smaller slope angle of PTES would decrease its thermal efficiency faster. However, the investigation time was as short as 40 min and could not demonstrate long-term reliability.

### 3.2. Numerical study for system integration

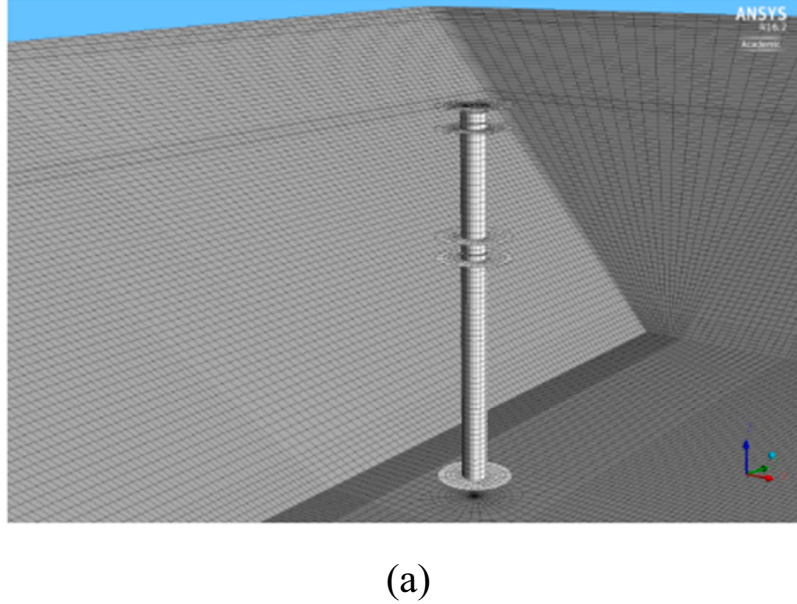
Future solar district systems will rely on variable renewable production and provide services for heating, cooling, and electricity [130]. Simulation and optimization should also be performed to ensure reliable design and operation of solar district heating systems integrated with PTES. Although such systems are highly dynamic and computationally complex, there is still some effort in the system-level investigation.

Reiter et al. [125] established the model of the Graz solar district heating plant using TRNSYS to predict the plant's performance while determining the optimum size of each component. Preliminary

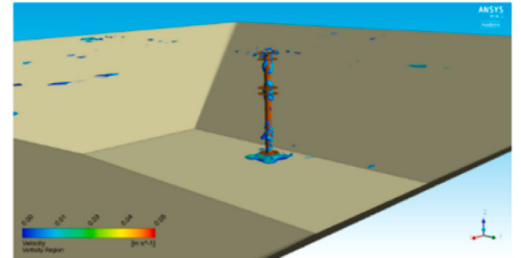
simulation results showed that the system had the best feasibility, with the solar collector field between 150,000 m<sup>2</sup> and 650,000 m<sup>2</sup>, and the solar fraction could reach 9 % to 26 %. However, the performance and economic potential of the plant were affected by many parameters. Therefore, detailed simulations need to be done to clarify all relevant parameters further.

Sorknæs [109] presented a mathematical method in an excel spreadsheet to simulate the operation of PTES combined with a heat pump of the Dronninglund solar district heating plant. The model provided a tool that was sufficient to approximate the energy flow between components closely. However, the variation trend of the internal temperature of the PTES was quite different from the measurement, and the heat loss was overestimated by 36.5 % compared with the actual operation. This was mainly due to the following simplifications: (1) The bottom temperature inside the PTES was set to be constant according to the operation period and the top temperature during the summer period. (2) The thermal exchanges between the soil and PTES were simplified by setting the soil temperature as constant all the year. (3) The fuel boiler provided a heat source to the heat pump was operating at full load.

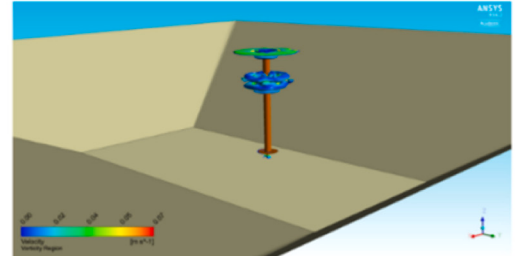
Li et al. [119] set up a solar heating system with PTES in Hebei, China. Meanwhile, a TRNSYS model calibrated by the experimental data



(a)



Discharge case on October 7



Charge case on August 3

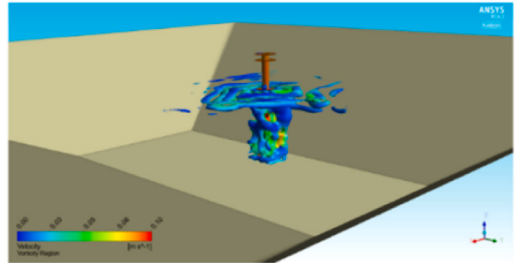
Discharge case on February 18  
(b)

Fig. 15. (a) Geometry and meshes for CFD model in Marstal [124]; (b) Illustration of regions for different cases [123].

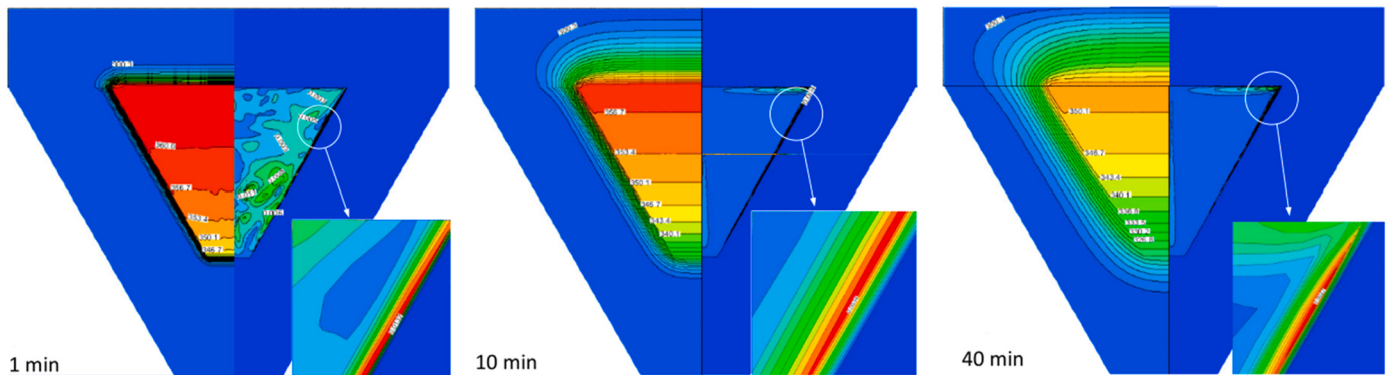


Fig. 16. Isotherms and streamlines distributions on cross-section over time [122].

was established. The study was mainly focused on comparing three control strategies (i.e., constant flow control strategy, temperature difference control strategy, and variable flow control strategy) between the solar receiver and PTES. By comparing simulation and measurement results, it was found that a better stratification inside the PTES could be achieved in a variable flow control strategy. A reasonable control strategy was of extraordinary significance in improving the system efficiency since it could increase solar collection efficiency and enhance the exergy efficiency of the thermal energy storage. Nevertheless, the system scale was small compared to solar district heating plants, and the

model for PTES was limited to tank storage. The research method can be considered a reference.

Narula et al. [113] developed a mathematical method to assess the hourly energy flow in a solar district heating system. Four configurations with different components could be considered. Simulation results were compared with the Marstal project for the configuration that included thermal energy storage and a heat pump (seen Fig. 17 [113]). Based on the validation with the measured values, the annual energy flow could be closely replicated, demonstrating that the tool provided a simple alternative to preliminary evaluate the solar district heating system's

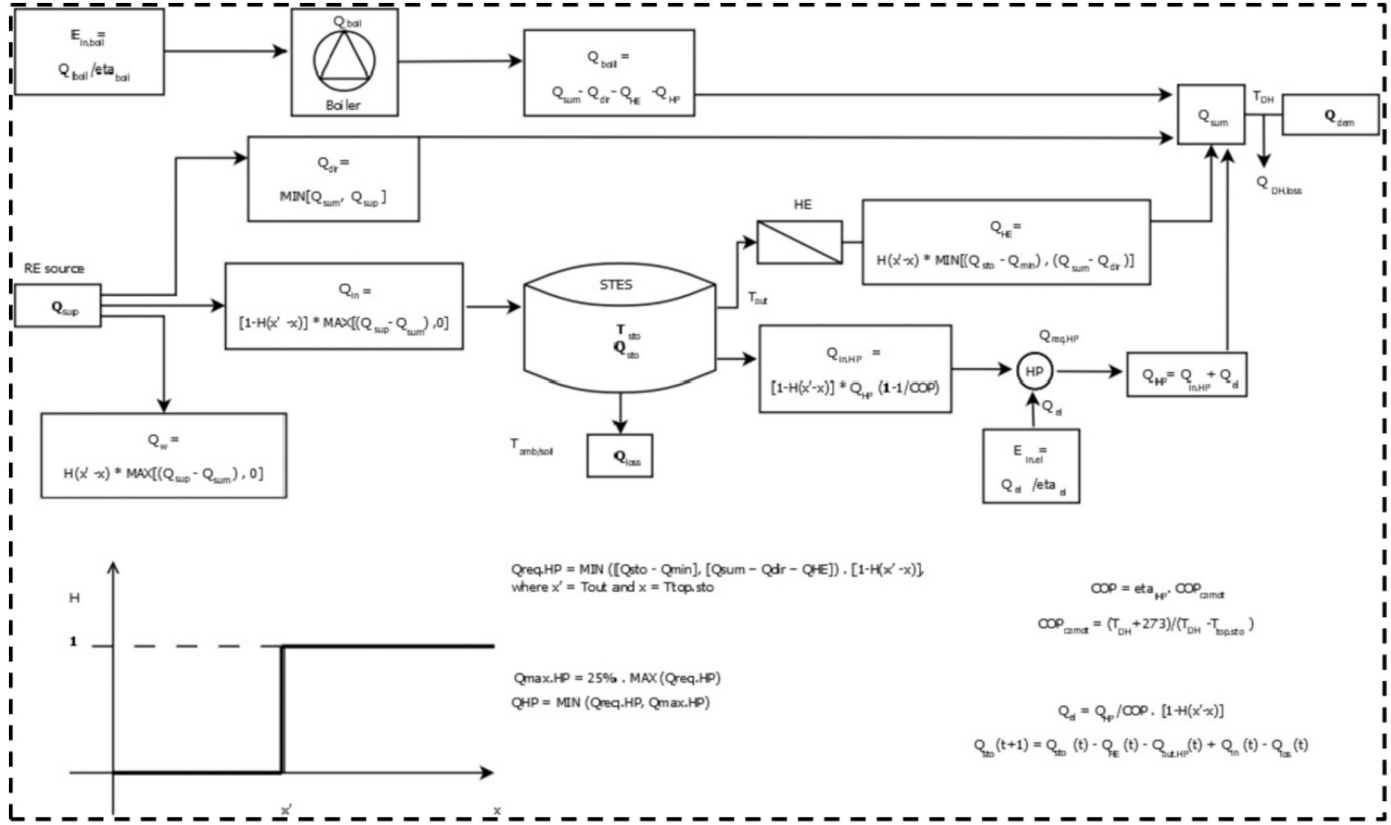


Fig. 17. System framework with a renewable source, a boiler, a thermal storage, a heat exchange, and a heat pump [113].

yearly energy flow. However, the monthly energy flow deviations of different components were quite large. Two reasons could explain this. First, the energy supply and demand profiles used as input were incorrect. Second, the PTES was neither fully charged nor discharged due to the operation control strategy. To conclude, the developed model could not replace the specialized software, primarily detailed investigations. Further modification and exploitation need to be done to improve the model.

Nageler et al. [120] developed a co-simulation framework shown in Fig. 18 [120], which coupled with different tools (DYMOLA, IDA ICE, and TRNSYS) to assess energy supply. DYMOLA was used for the heating network simulation, IDA ICE was used for the building and substation simulation, and TRNSYS was used for the energy supply system simulation. Six cases were carried out to evaluate the tool, of which two cases included PTES aimed to overcome the seasonal fluctuating of waste heat. The co-simulation framework was reliable based on a virtual solar district heating system simulation. Significantly, the utilization of PTES was proved to be an effective way to balance the seasonal fluctuating waste heat. Moreover, climate conditions needed to be heavily considered to avoid oversizing the system components. This paper proposed a new way to evaluate the energy system by utilizing the advantages of different software. However, the accuracy needs to be further verified by comparing it with actual projects.

Kubinski and Szablowski [114] developed a simplified dynamic model in the ASPEN HYSYS software based on the existing installation of the Vojents project. The model consisted of the collector field loop, the PTES application loop, and the heat distribution loop. The proposed model was expected to assess the achievable solar fraction. However, the simulation results, such as the solar fraction and water temperature distribution inside the PTES, differed significantly from the actual projects due to assumptions about the PTES and the system control strategy. It was recommended to change the software to TRNSYS, considering the inaccurate results, so that problems encountered in the proposed model,

including missing components, detailed boundary conditions, and the time-varying parameters, can be easily resolved.

### 3.3. Summary and outlook on PTES numerical studies

#### 3.3.1. Model classification and model accuracy

The aforementioned numerical approaches can be classified in Fig. 19, where the thickness of curve between platform and dimension represents the current research proportion of each source item. As an illustration, about 50 % of the research conducted on FLUENT uses three-dimensional modes, 40 % uses two-dimensional models, and the other 10 % uses one-dimensional models.

Fig. 19 shows that different simulation approaches have their characteristics and applicability. Recently research on PTES has concentrated on the TRNSYS platform, and the model dimensions are mostly one-dimensional and two-dimensional. In addition, it clarifies that not all geometries can be implemented in the current one-dimensional and two-dimensional models, bringing potential avenues for future research. Although FLUENT is known to implement various complex requirements, it is less utilized due to high time consumption. It is worth noting that the groundwater effect is only considered by Dahash et al. [118,131] successfully in a two-dimensional model. However, the asymmetric effect of groundwater in the two-dimensional model will be ignored, so its three-dimensional features need to be further corrected.

It is also valuable to compare the calculation accuracy of previous studies. Therefore, three indicators of annual deviation, maximum monthly deviation, and maximum temperature difference are used to compare the different numerical models. Fig. 20 plots the relevant results from previous studies, where the models implemented in the TRNSYS platform are shown with a grey and white background, the model implemented in the COMSOL platform is shown with a pink background, and the models implemented in the FLUENT platform are shown with a brown background.

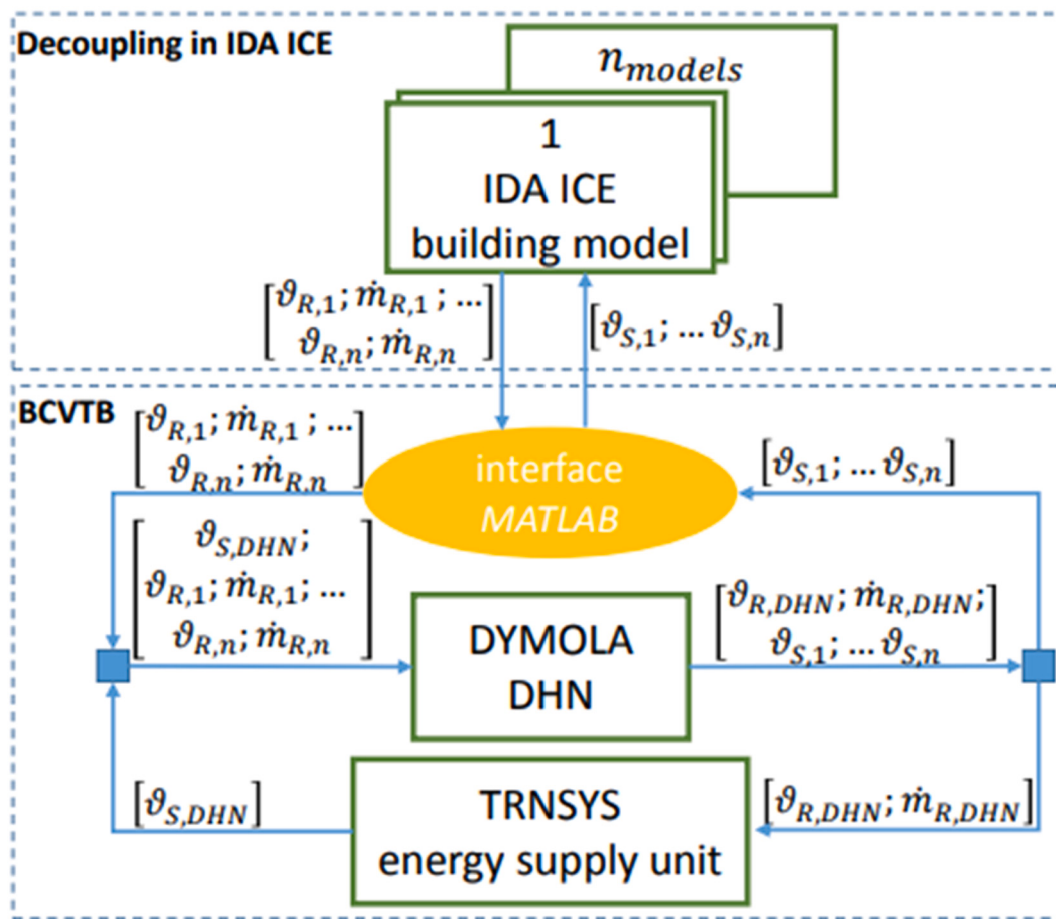


Fig. 18. Co-simulation framework [120].

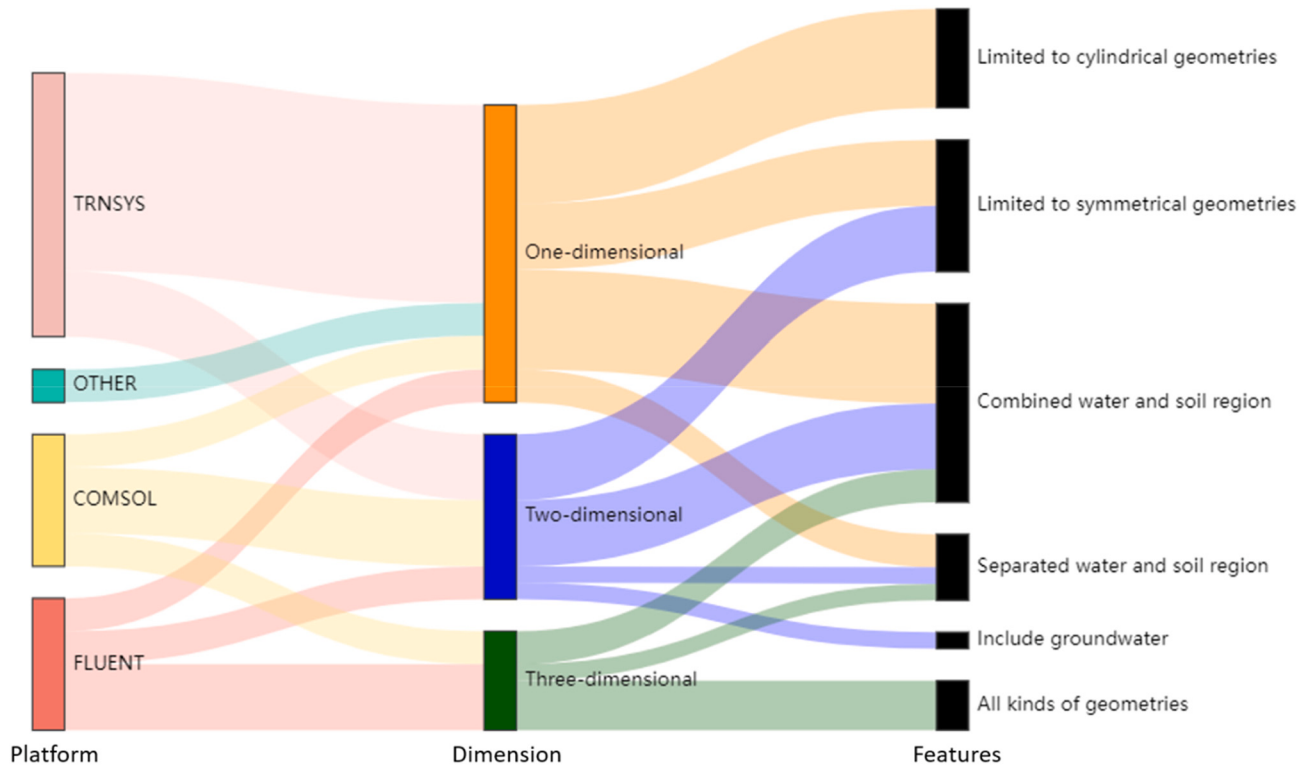
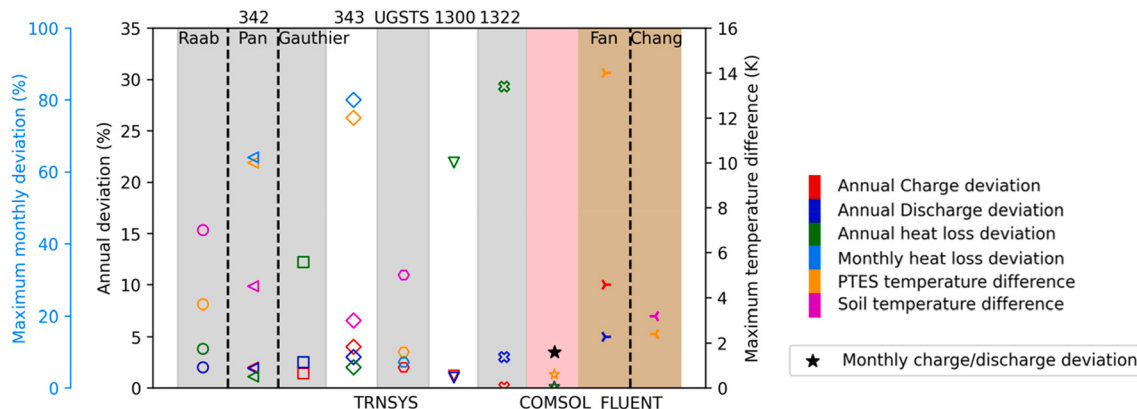


Fig. 19. Classification of recent simulation approaches for PTES.



**Fig. 20.** Numerical model calculation accuracy in previous studies [24,110–112,116,122,123,127].

As shown in Fig. 20, all the numerical models have good calculation accuracy regarding annual charge and discharge energy, with the annual deviations within 5 %. However, some studies found large deviations beyond 10 % in annual heat loss. It is important to note that even with the same model, there are significant differences in the annual heat loss calculation, which may be due to the settings of boundary conditions, including initial soil temperature, soil physical parameters, and heat transfer coefficients between water and soil. Moreover, three previous studies found large deviations in monthly calculations. The charge/discharge energy deviation in Fan's study is also an instantaneous result, as employing FLUENT for long-term simulations is challenging.

For calculation accuracy of PTES and soil temperature, there are considerable differences between different models. For one reason, a limited number of nodes are set using TRNSYS models in earlier studies. Another reason is that the relative position of soil measurements to the PTES walls changes after the PTES is transformed into cylinder geometry.

In conclusion, in the previous research, the model implemented on the COMSOL platform demonstrated good computational accuracy in all aspects. However, the model built based on COMSOL is not easy to link to system simulation software like TRNSYS. Furthermore, it is preferable to use the same setting to evaluate the suitability of various models further.

### 3.3.2. Model assumptions

Numerous assumptions are used in different numerical models in an effort to improve computational efficiency. As discussed above, the calculation accuracy is acceptable for annual simulation. Still, more significant deviations appear when comparing the monthly or daily results with measurements since not all assumptions in the models are fully met in the actual project [7].

Table 5 summarizes the commonly adopted assumptions and categorizes them according to the aspects they consider. It is essential to point out that one of the common assumptions is axisymmetric flow and heat transfer. In this context, the temperature distribution inside the PTES and the heat loss through the sidewalls can be misleading without considering the asymmetrical flow and heat transfer. The plug flow assumption is widely used in most simulation platforms without considering the inlet/outlet mixing. Moreover, the FLUENT platform commonly assumed a laminar flow inside PTES to achieve a stable and faster simulation. However, no studies have shown that more precise results can be obtained with the laminar flow than with turbulent flow.

### 3.3.3. Model correlations

Four primary corrections are tried in recent numerical models to overcome the disadvantages caused by the assumptions, and eventually improve the calculation accuracy. They are: (1) heat transfer coefficient of the surfaces; (2) eliminate inverse thermocline; (3) minimize numerical diffusion; (4) influence of groundwater.

**Table 5**  
Main assumptions adopted in PTES numerical models.

Aspects	TRNSYS	FLUENT	COMSOL	Others
Dimensional problem	Axisymmetric flow and heat transfer		Axisymmetric flow and heat transfer	Axisymmetric flow and heat transfer
Water properties	Constant thermal conductivity		Constant thermos-physical properties	Constant thermal conductivity
Soil properties	Constant thermos-physical properties	Constant thermos-physical properties	Constant thermos-physical properties	Constant thermos-physical properties
Heat transfer fluid from inlet/outlet diffusers	Neglect inlet mixing effect			Neglect inlet mixing effect
Heat transfer mechanism of water region	Neglect radial density gradients The water of each layer was considered thoroughly mixed before entering the adjacent layer Temperature inversion is not allowed Uniform temperature distribution of each layer Plug flow Uniform initial temperature	Laminar flow	Neglect radial density gradients The water of each layer was considered thoroughly mixed before entering the adjacent layer Uniform temperature distribution of each layer Laminar flow	Neglect radial density gradients Uniform temperature distribution of each layer Plug flow
Heat transfer mechanism of soil region	Neglect the influence of groundwater Uniform initial temperature	Neglect the influence of groundwater		Neglect the influence of groundwater
Heat transfer mechanism between soil and water region	Simplify the influence of natural convection			Neglect the influence of natural convection

### (1) Heat transfer coefficient of the surfaces

The surface area of the PTES in the TRNSYS models differs from the surface area in reality since the actual shape needs to be converted to a cylinder or a reversed truncated cone in these models. In this case, a calculation error of heat loss will be introduced. Thus, to account for the surface variation, the heat transfer coefficient is corrected as Eq. (1) [112,117].

$$U_{\text{simulation}} = U_{\text{original}} * \frac{A_{\text{original}}}{A_{\text{simulation}}} \quad (1)$$

where the  $U_{\text{simulation}}$  and  $U_{\text{original}}$  represent the surface heat transfer coefficient for the modeled PTES and the original PTES, respectively.  $A_{\text{simulation}}$  and  $A_{\text{original}}$  are the corresponding areas of the modeled PTES and the original PTES respectively.

However, some researchers use actual measurement results as constraints to obtain  $U_{\text{original}}$ , and some researchers assign  $U_{\text{original}}$  empirically. Consequently, the deviation of monthly heat loss is relatively large. Furthermore, during the planning phase, the heat transfer coefficient is unknown. Therefore, research is needed to propose an empirical formula suitable for different geological conditions.

### (2) Eliminate inverse thermocline

Due to heat loss, a temperature drop may be observed at the very top layer near the cover. This drop may create an undesirable phenomenon called ‘thermocline inversion’. To eliminate this, three methods have been used in recent approaches. The first method is to swap two adjacent nodes, which is suitable for the case where the volume of each node is equal. However, this method may introduce large errors when dividing PTES (with unequal top and bottom cross-section areas) into nodes of equal height. Thus a second method is proposed in several TRNSYS models, which defines a mixed temperature according to Eqs. (2) and (3). When the thermocline inversion occurs, the temperature is replaced by the mass average temperature of the two adjacent nodes.

$$T_{\text{mix}} = (T_i * C_{p(i)} + T_{i+1} * C_{p(i+1)}) / (C_{p(i)} + C_{p(i+1)}) \quad (2)$$

$$T_i = T_{i+1} = T_{\text{mix}} \quad (3)$$

However, this method deviates from the reality and miscalculates the heat loss through the sidewalls. Then, another method proposed by Dahash et al. [117] argued that correcting the thermal conductivity of water could better address this issue. Accordingly, the enhanced water thermal conductivity can be expressed as Eq. (4).

$$\lambda_{w,\text{enh}} = C^* \left( \frac{\partial T_i}{\partial z_i} \right)^k \quad (4)$$

Both  $C$  and  $k$  are two constants that are usually determined experimentally.  $C$  is related to the dimensional parameters and thermophysical properties, and  $k$  depends on the application situation.

### (3) Minimize numerical diffusion

For the one-dimensional models, the water region will be divided into several nodes in the vertical direction. The water temperature of the entire node near the inlet will be replaced by the thoroughly mixed average temperature of incoming water and existing water. Then, due to the plug flow assumption, artificial mixing will spread throughout the entire water region under different time steps. That causes significant numerical diffusion, especially when the mass per node is greater than the mass inlet flow within a time step.

In order to minimize the influence of numerical diffusion, two methods are generally adopted. One way is to increase the number of nodes, which can produce similar results to the actual situation. However, there is no straightforward rule for finding the appropriate number of nodes influenced by the storage dimensions and the operating condition. Furthermore, a large number of nodes may be required in some cases, which is undesirable due to a high computational cost.

The alternative way is the introduction of a virtual tank with a volume equal to that of the layer [132]. This method works only if all the

layers have an equal volume. It assumes that the incoming water accumulates in the virtual tank first. When the virtual tank is full, all the accumulated water in the tank enters the storage node with the inlet [133]. Bai et al. [116] compared the influence of the plug flow method and found that the node's size still needed to be adjusted since it was related to the virtual tank's volume. Therefore, when water with significant temperature differences in multiple time steps is mixed in the virtual tank, the predicted temperature will also significantly differ from the experimental results.

### (4) Influence of groundwater

Awareness of the important impacts of groundwater on the planning and construction of PTES is increasing significantly. One concern is that groundwater challenges the excavation techniques and increases the construction investment. Another concern is that increased heat losses from the side and bottom walls of PTES will increase due to the enhanced heat transfer caused by groundwater. Additionally, significant temperature increases in the groundwater due to heat transfer from the water area may deteriorate groundwater quality [131]. However, most of the works discussed above neglect groundwater due to the model complexity.

Still, two efforts have been attempted to include the groundwater effect in the models. One attempt was to stratify the soil in height by different soil properties. In other words, the soil part with groundwater has a higher thermal conductivity. Yet, the soil properties of each layer of this method are still uniform without considering the groundwater flow. In this case, the interaction of PTES and groundwater cannot be predicted.

Another attempt was to take into account the hydraulic process of groundwater by introducing Darcy's law into the model. As proposed by Dahash et al. [131], the heat transfer equation in the soil layers was revised as Eq. (5).

$$(\rho c_p)_{\text{eq}} \frac{\partial T}{\partial t} + \rho_{\text{gw}} c_{p,\text{gw}} u^* \nabla T = \nabla^* (\lambda_{\text{eq}} \nabla T) \quad (5)$$

where  $(\rho c_p)_{\text{eq}}$  and  $\lambda_{\text{eq}}$  are the equivalent volumetric heat capacity and thermal conductivity of the porous medium in which the groundwater flows.  $\rho_{\text{gw}}$  and  $c_{p,\text{gw}}$  represent the density and specific heat capacity of the groundwater respectively.

The second method can better predict the interaction between the groundwater and the PTES. This method can be implemented more easily on the COMSOL platform but is problematic in TRNSYS.

### 3.3.4. Outlook of numerical studies on PTES

Overall, the research stage of numerical studies for PTES has not yet reached a mature level. Therefore, there are several potential directions for future research in the numerical analysis of PTES, especially in developing sophisticated models that take into account geometrical suitability and geological conditions or in making full use of characteristics of different simulation platforms to improve the accuracy of existing models.

Few numerical studies have been conducted on PTES-integrated solar district heating systems. PTES complicates the operation of solar district heating systems. Consequently, there is a strong need for system-level investigation to determine the optimum system design and operation strategy [134].

## 4. Application of PTES

The first PTES with a volume of 500 m<sup>3</sup> was constructed at the Technical University of Denmark and extensive investigations were carried out [135–138]. The experience gathered from this project served the basis for constructing large-scale projects in Denmark and inspired the solar heating industry to establish more plants with PTES [139]. More recently, connecting PTES to large-scale solar district heating system has become one of the premier technologies to address the issue

of solar thermal time-discrepancy. Although technical and economic viabilities have been successfully demonstrated, only a small fraction of its potential has been exploited. To give a global perspective of PTES application, statistics on the application of PTES are essential.

#### 4.1. Worldwide distribution

**Fig. 21** illustrates the global contribution of large-scale solar district heating systems with PTES, highlighting PTES-active nations in different colors based on the number of publications. Over the past ten years, researchers in China and Austria produced more than ten articles, demonstrating the highest level of interest, followed by Denmark, Germany, Switzerland, and the United States.

Moreover, as the number of systems marked in **Fig. 21**, countries have effectively integrated PTES into solar district heating plants, with Denmark accounting for around 47 % of these installations, Germany 40 %, and Sweden and China 13 %. Together with **Table 6**, which summarizes the technical specifics of 15 solar district heating plants with PTES (PTES volume > 500 m<sup>3</sup>), Denmark has emerged as a leader in the use of PTES, with significant growth in the installation of PTES reported over the past years. However, countries actively researched in the early years, such as Sweden and Germany, are now lagging.

Furthermore, the first solar heating plant with PTES in China was successfully realized in 2018 under severe weather conditions, thanks to the Danish PTES technology. In Austria, no PTES system has been built, but as far as we know, one is being planned. Due to the promotion of energy storage policy and the rising number of academics attempting to assess the technical feasibility and potential obstacles, more projects are anticipated in these two countries.

Planning and implementing PTES integration on such a large scale is problematic because it faces numerous challenges frequently. Despite the recent significant discrepancy in PTES worldwide, the application of PTES is moving from demonstration to commercialization, and the number of PTES is expected to increase in the future.

#### 4.2. Classifications of PTES connected to solar district heating systems

**Fig. 22** shows four classification categories for PTES connected to

solar district heating systems: storage material, construction type, operation strategy, and application method, according to **Table 6**.

The first criterion is indicated in **Fig. 23**. Earlier projects, like those in Lambohov, Stuttgart, Augsburg, Steinfurt, Chemnitz, and Eggenstein, commonly used gravel&water as storage material. However, it was replaced by water in the new projects for three reasons. One reason is that gravel&water have a lower energy density than water. The second reason is the requirement for indirect heat exchange coils of gravel&water PTES for charging and discharging, which add complexity to the system and is inconvenient to maintain. In addition, water can maintain an excellent thermal stratification [5,73]. It is worth noting that, depending on the quality of the steel used, water may need to be treated after filling to prevent corrosion. Typically, if steel is utilized for the metal components of the PTES, the pH value of water will be raised to roughly 9.8 [5,20,44,72,73].

The second criterion is represented in **Fig. 24**. PTES volumes for projects before 2008 were completely buried under the ground level (see **Fig. 7** (a)) since their volumes were small, and their depths were all <7 m. However, as newly built PTES increases in volume and becomes deeper, the PTES is partly buried, and the above-ground part is supported by embankments made of the excavated soil (see **Fig. 7** (b)). In this case, heat losses due to groundwater are avoided through the sidewalls. To our knowledge, the sidewalls of PTES can account for around 40 % of the heat loss [112], primarily due to groundwater effects, which increase further [15,16]. Therefore, an in-depth geological investigation is recommended before the construction of PTES.

The third criterion, PTES operates with/without a heat pump, is displayed in **Fig. 25**. For systems without a heat pump, the minimum PTES temperature is around 20 °C. However, in systems with a heat pump, the heat pump extracts heat from the PTES to lower the minimum temperature to 10 °C when the temperature inside the PTES is not high enough for direct heating. Therefore, the storage efficiency can be improved by using the heat pump property in this situation [153–158]. The achievement of lower storage temperature also allows for a reduction in heat losses.

Notably, the choice of the heat pump depends on the local energy structure and policy. The proportion of renewable energy share in the solar district heating systems can be increased with careful heat pump

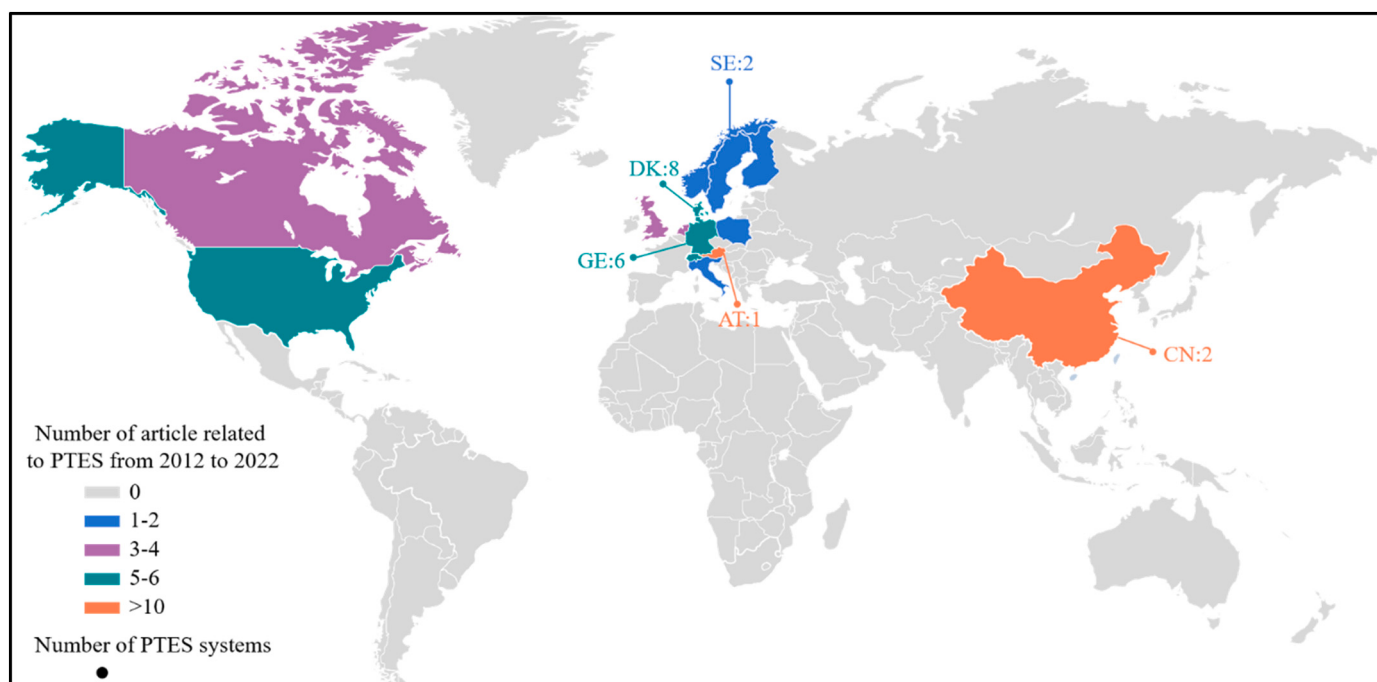


**Fig. 21.** Global scientific publications on solar district heating plants with PTES.

**Table 6**Detail information of PTES projects (PTES volume > 500 m<sup>3</sup>).

Position	Country	Year	Solar collector field area (m <sup>2</sup> )	PTES volume (m <sup>3</sup> )	Buffer tank volume (m <sup>3</sup> )	Heat pump (type/capacity (kW))	Auxiliary energy (type/capacity/number)	Heat demand (MWh)	References
Lambohov Stuttgart	Sweden Germany	1980 1985	2700 211	10,000 1050	— 1	Compression/— Compression/66	Gas Boiler/—/1 Co generation plant/—	900 100	[140–142] [32,33,143]
Julich	Germany	1996	1200	2500	1–2	—	Gas Boiler/750 kW/1	590	[140,144]
Augsburg Steinfurt Chemnitz Eggenstein	Germany Germany Germany Germany	1996 1999 2000 2008	2000 510 2000 1600	6000 1500 8000 4500	— 1000 — 30	— — — Compression/60	Gas Boiler/—/1 Gas Boiler/—/1 Gas Boiler/—/1 Gas boiler/600 kW/2	— 325 1200 1400	[35,36,143] [11,24,38,140,143–145] [24,31,35,36,143,146,147] [24,27,39,40,143]
Herlev	Denmark	1991	1050	3000	10	Compression/—	Gas boiler/—/1 Gas CHP/—/1	—	[74,143,148]
Ottrupgård Marstal	Denmark Denmark	1995 2012	560 33,300	1500 75,000	— 2100	— Compression/ 1500	— Biomass boiler/4 MW/1 Bio-oil boiler/8.3 MW/1 ORC/750 kW/1 Bio-oil boiler/5 MW/1 Bio-oil boiler/10 MW/1 Gas boiler/8 MW/1 Gas CHP/1.6 MW/1	43.5 32,000	[44,140] [28,41,42,45,77,148,149]
Dronninglund	Denmark	2014	37,573	60,000	None	Absorption/4700	Bio-oil boiler/5 MW/1 Bio-oil boiler/10 MW/1 Gas boiler/8 MW/1 Gas CHP/1.6 MW/1 Electric boiler/10 MW/1 Gas boiler/5.5 MW/1	40,000	[4,28,46,149,150]
Gram	Denmark	2015	44,000	122,000	2300	Compression/900	Gas CHP/5 MW/ 6MWth/1 Industrial surplus heat/2 MW	30,000	[10,48,151,152]
Vojens	Denmark	2015	70,000	200,000	—	Absorption/5100	Electric boiler/10 MW/1 Gas boiler/5.5 MW/ 1 Gas CHP/5 MW/ 6MWth/1 Industrial surplus heat/2 MW	28,000	[50–52]
Toftlund	Denmark	2017	27,000	70,000	—	Absorption/5100	Electric boiler/3 MW/1 Gas boiler/4.5 MW/ 1 Industrial surplus heat/1500– 4000MWh/year	28,000	[53–55]
Langkazi Tibet	China	2018	22,275	15,000	None	—	Electric boiler/1.5 MW/2	37,300	[56,57]

type selection. However, some researchers have pointed out that introducing heat pumps may not always help improve the overall energy perspective [159]. Thus, additional investigations are still needed to determine the optimum design and operation strategies for integrating heat pumps with PTES.

The fourth criterion of the PTES application method is shown in Fig. 26. PTES has traditionally been proposed for long-term storage due to its large size. The primary processes for charging and discharging occur in summer and winter, respectively. As a result, an additional buffer tank is required to account for short-term variation in heat demand. However, in addition to the seasonal storage process from summer to winter, PTES can also be employed as short-term storage in summer [46]. In this context, storage efficiency is improved, and heat loss is reduced, as the average PTES temperature during summer is lower than that of the traditional application method. Additionally, the investment in the buffer tank can be saved.

#### 4.3. Operation status of solar district heating plants with PTES

Integrating PTES into a solar district heating system has many advantages, such as achieving higher solar fraction and system efficiency. However, only 15 of the 470 large-scale solar district heating systems that have been successfully implemented worldwide integrated with PTES, which means the application of PTES remains challenging. The system will be more complicated than a system without PTES, and the desired efficiency may only be achieved with proper design and operation strategies [130,160]. In order to comprehend the operating statistics of existing PTES applications, and understand the current technical barriers and successful experiences, the project performance indicators, successes, and failures are presented in Table 7. Based on Table 7, Fig. 27 provides a comparison of performance metrics regarding solar fraction, storage efficiency, storage cycle, and PTES temperature.

As can be observed in Fig. 27, the majority of projects have solar fractions between 30 % and 50 %, while the Lambohov and Langkazi Tibet projects have solar fractions exceeding 60 %. Solar fraction is defined as the percentage of the total thermal load satisfied by solar

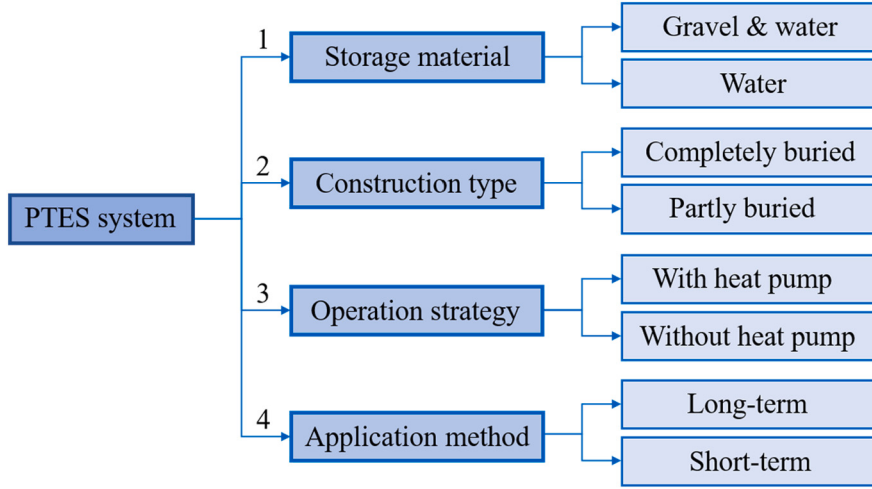


**Fig. 22.** Classification categories of PTES connected to solar district heating systems.

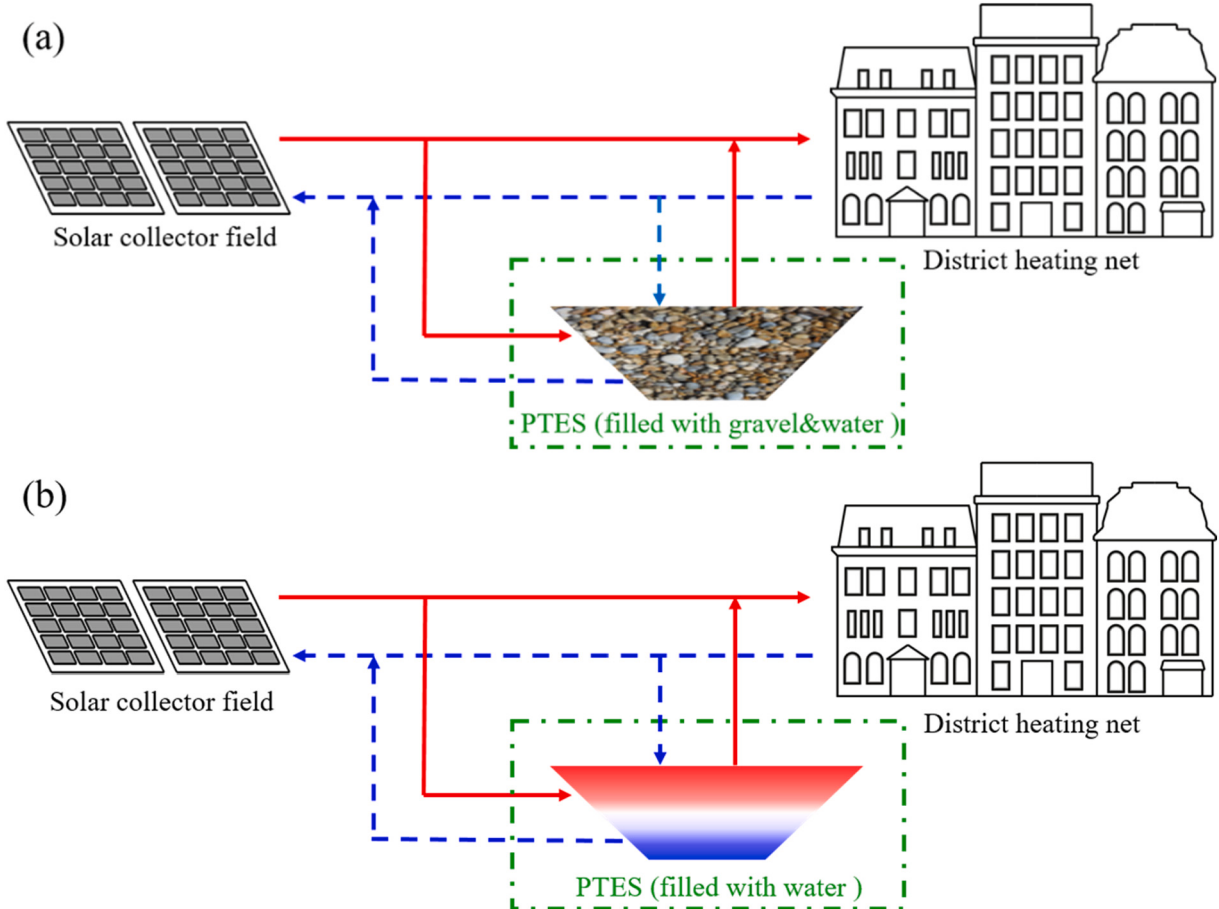


**Fig. 23.** Criterion 1: storage material filled inside PTES: (a) filled with gravel & water; (b) filled with water.

energy. Therefore, the operational strategy and component design will both affect solar fraction. In the Stuggart and Tibet projects, the solar collector fields are slightly oversized, wasting extra heat during certain summer months. Notably, the Marstal project's solar fraction in 2017 fell below 30 %. The reason is that rainwater has entered the cover construction through leakage, increasing the humidification of the cover and further increasing the heat loss through the cover.

In terms of storage efficiency, a significant gap can be observed. There are several points to be clarified. The ratio of the sum of the

discharged and internal energy changes to the charged energy is known as storage efficiency. For the Dronninglund PTES, storage efficiency has increased slightly yearly, peaking at 96 % in 2017. The higher storage efficiency, when compared to Marstal and Gram, is partly attributable to the storage cycle, which is defined as the ratio of the discharged heat to the maximum heat capacity of PTES. As demonstrated in Fig. 27, Marstal and Gram have storage cycles lower than 1, while the typical storage cycle for the Dronninglund project lowers the minimum PTES temperature to

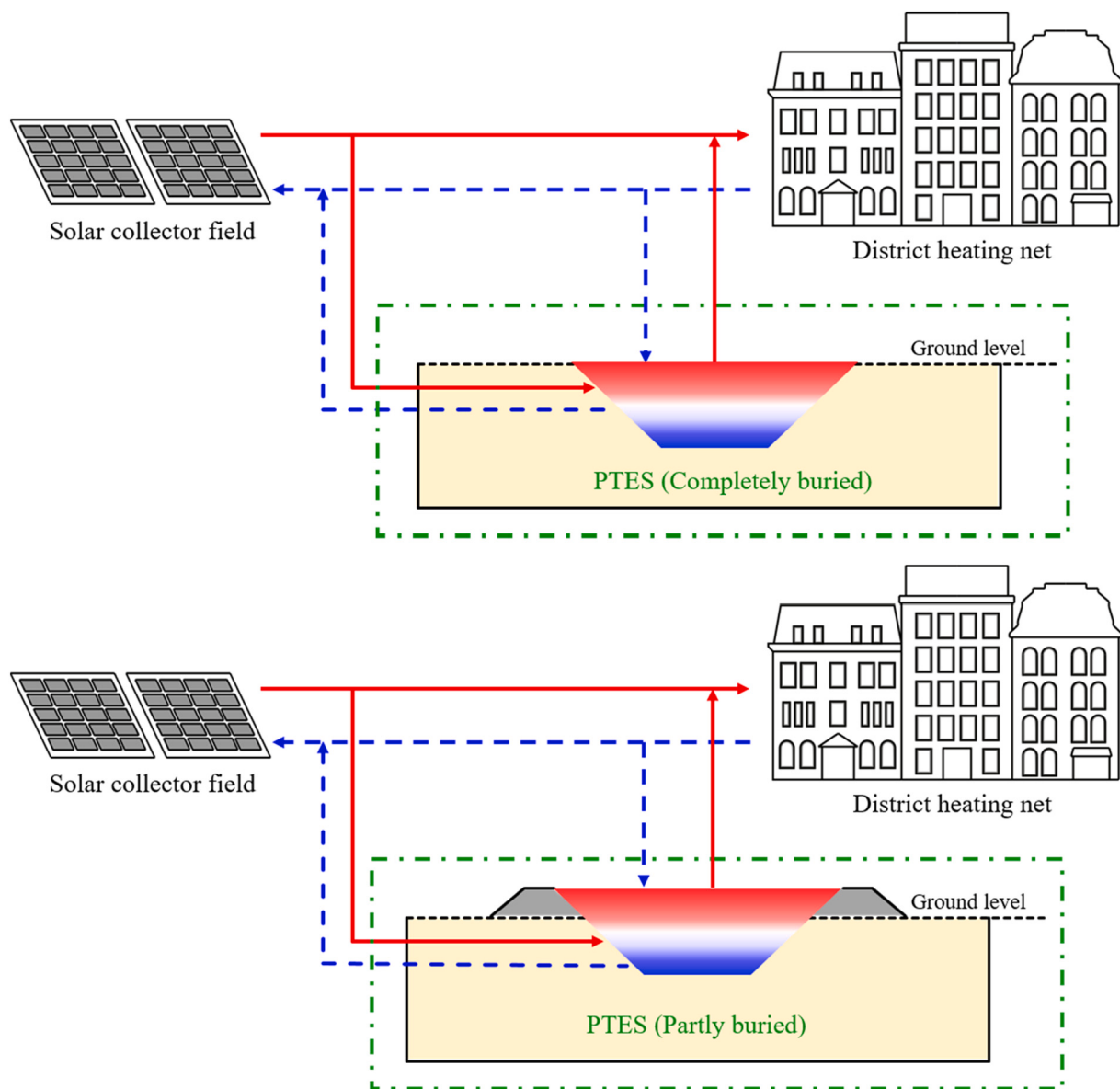


**Fig. 24.** Criterion 2: construction types of PTES: (a) completely buried; (b) partly buried.

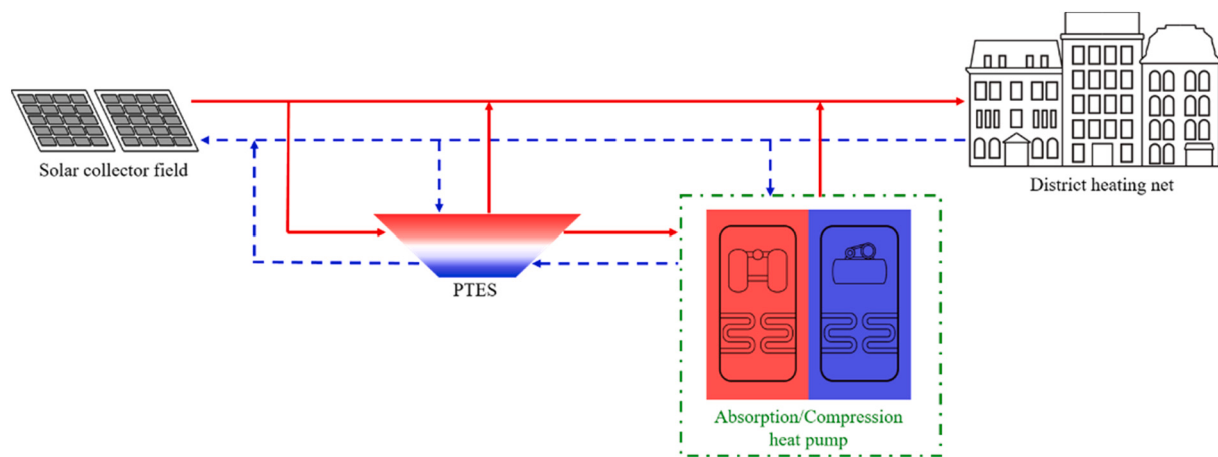


**Fig. 25.** Criterion 3: operational strategy.

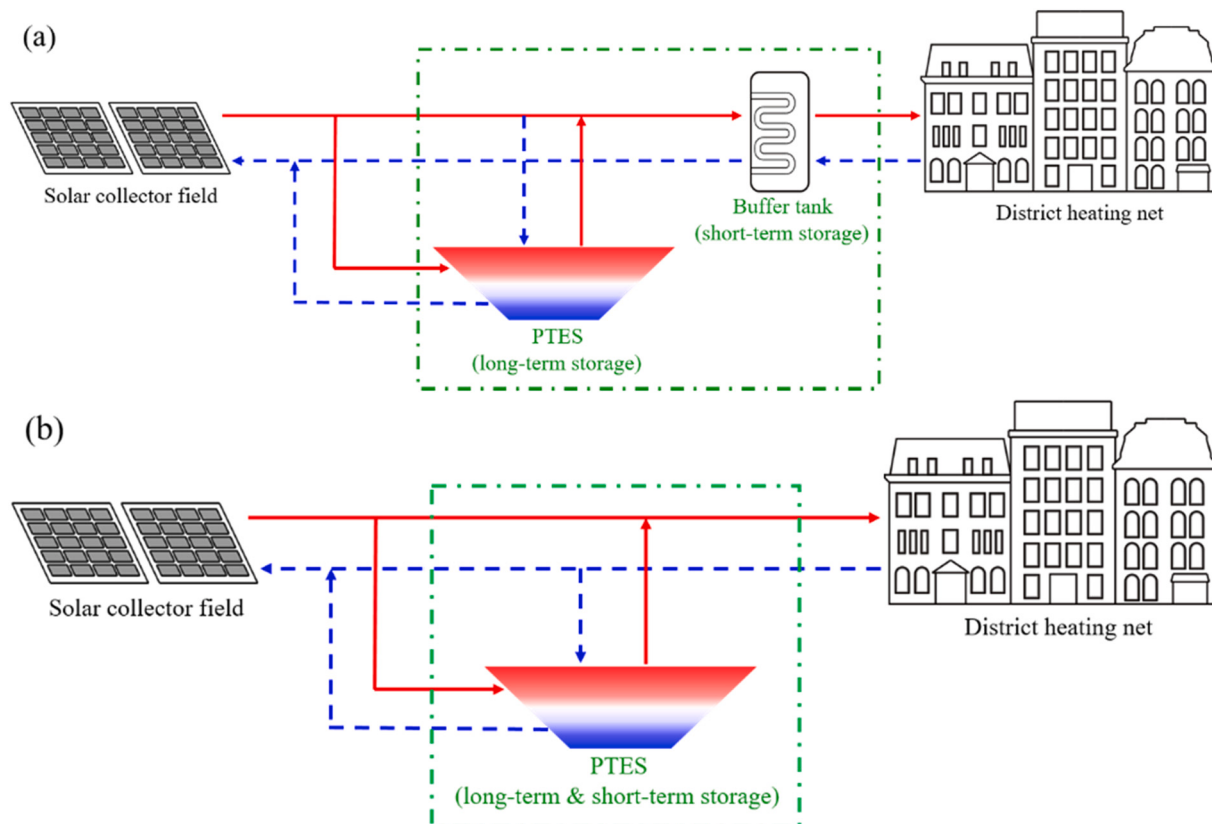


**Fig. 26.** Criterion 4: application method of PTES: (a) long-term; (b) short-term.

approximately 10 °C, reducing the heat losses from the side and bottom walls. The beneficial effect of the storage cycle on storage efficiency can also be proved with the Stuttgart projects. Even though the storage temperature is limited to around 30 °C due to the use of unglazed collectors, the heat pump can fully utilize the storage capacity and achieve a large storage temperature difference.

#### 4.4. Summary and outlook of PTES application

As summarized in Table 7, successful projects demonstrated the applicability of PTES in different regions and climate zones. PTES can be seen as a major player in future district heating systems, incorporating a significant amount of renewable energy. In contrast, PTES grows in size to fulfill seasonal tasks, which brings more issues to the application. For instance, a thorough geotechnical and hydrogeological assessment is required prior to PTES construction. For larger volumes of PTES, a better cover design must be suggested to reduce heat loss and sustain service life. Additionally, the additional potential for using PTES when integrated with different system components is not reflected in current operational statistics. So it is necessary to explore the adaptability of the combination with different systems further.

#### 5. Conclusion and future research directions

PTES has attracted more and more attention. However, certain technical challenges that are not yet to be sufficiently covered have limited its rapid development. This paper has addressed three aspects, namely technical elements, numerical approaches and applications, which the authors believe will be the key drivers for the future development of PTES. The main findings and the challenges can be summarized as follows:

*Main findings*

- Due to the high energy density and ease of maintenance, 64.3 % of the analyzed projects use water as heat storage. 42.8 % of the analyzed projects are partly buried to avoid the groundwater level. In addition, 25.8 % of the analyzed projects use PTES for both long-term and short-term storage, which will improve storage efficiency by about 50 %. Moreover, 63.8 % of the analyzed projects are coupled with a heat pump, reducing the PTES minimum temperature to around 10 °C, further improving the storage efficiency by around 40 %.
- Due to the failure of cover design and construction, the design value of storage efficiency is commonly overestimated by 28 % or even as high as 46 %. In the past, the floating cover of PTES has caused technical problems and unnecessary heat loss (60 % of total heat loss), in the worst cases, accidents. Another important practical issue is that the mismatch between solar collector field design and PTES size leads to considerable energy waste in summer.
- At present, the maximum temperature of PTES is generally controlled below 85 °C because of a significant decrease in the lifetime of liner materials with temperatures higher than 85 °C.
- The existing numerical models for PTES are improved from four aspects: correcting the heat transfer coefficient between soil and water region, eliminating the inverse thermocline, minimizing the numerical diffusion, and considering the influence of groundwater. The prediction errors of different models for annual charged and discharged energy are within ±10 %.
- Simulation approaches for system integration are less studied, and most of the characteristic parameters such as solar fraction, total heat loss, and storage efficiency are significantly different from the actual projects due to the simplification of the operation strategy.

*Main challenges*

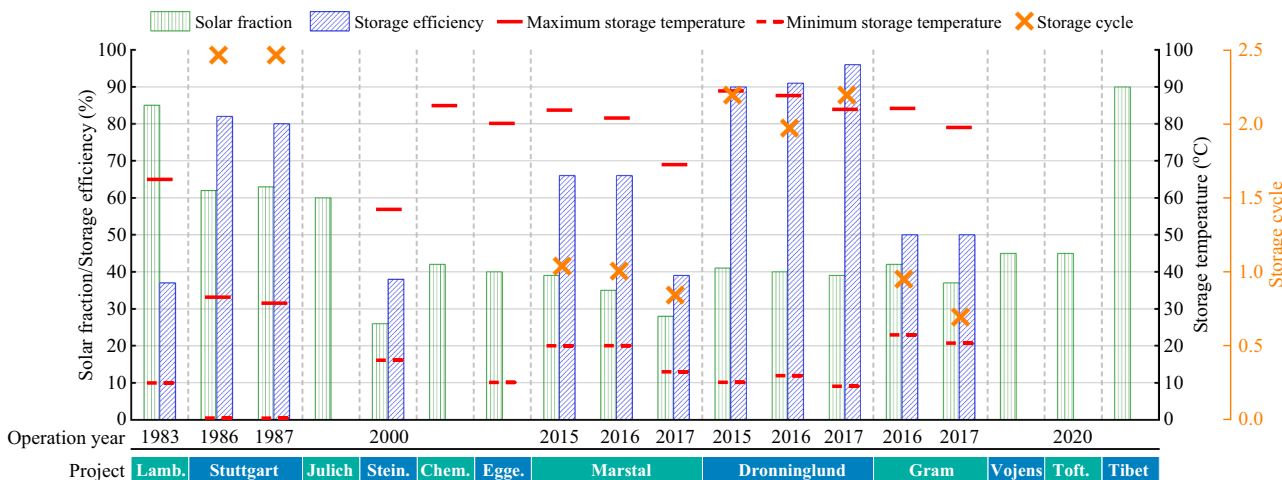
**Table 7**Operational statistics of available PTES projects (PTES volume > 500 m<sup>3</sup>).

Project	Solar fraction	Storage efficiency	Number of storage cycles	Storage max/min temperature (°C)	Storage heat loss (MWh)	Success experience	Failure experience	References
Lambohov	85 %	37 %	–	65/10	395 (1983)		<ul style="list-style-type: none"> <li>• Large heat loss due to wet insulation</li> <li>• No proper tools for predesign</li> <li>• Heat pump not working as expected</li> <li>• Unglazed collectors cannot provide higher temperatures to increase the storage efficiency</li> <li>• Large energy waste from collectors</li> <li>• Solar fraction of operation is 18.9 % lower than the design value</li> <li>• Leakage at the welded part of the sealing foil</li> <li>• High investment</li> <li>• Increase moisture content of insulation due to drain pump failure</li> <li>• Storage efficiency of operation is 45.7 % lower than the design value</li> <li>• Excavated with vertical walls accounts for a large part of the cost</li> </ul>	[141,161]
Stuttgart	62 % (1986) 63 % (1987)	82 % (1986) 80 % (1987)	2.4 (1986) 2.4 (1987)	33/0 (1986) 31/0 (1987)	11.7 (1986) 13 (1987)	<ul style="list-style-type: none"> <li>• PTES used as heat and cold storage</li> <li>• Water is well maintained, free from fouling and corrosion</li> </ul>		[32,141]
Julich Steinfurt	60 % 26 % (2000)	– 38 % (2000)	–	– 67/10 (1999) 57/16 (2000)	– 80 (2000)			[144] [38]
Chemnitz	42 %	–	–	85/	–			[31,147]
Eggenstein	40 %	–	–	80/10	–	<ul style="list-style-type: none"> <li>• Successful heat pump operation strategies increase the efficiency of PTES</li> </ul>		[11,31]
Herlev Ottrupgård	– –	– –	– –	85/10 60/35	– 70			[165] [43]
Marstal	39 % (2015) 35 % (2016) 28 % (2017)	66 % (2015) 66 % (2016) 39 % (2017)	1.1 (2015) 1.0 (2016) 0.7 (2017)	84/20 (2015) 82/20 (2016) 69/13 (2017)	2626 2424 4155	<ul style="list-style-type: none"> <li>• Backup boilers operate on the bio-oil enabling system to be 100 % renewable energy</li> </ul>		[28,149,162]
Dronninglund	41 % (2015) 40 % (2016) 39 % (2017)	90 % (2015) 91 % (2016) 96 % (2017)	2.2 (2015) 1.9 (2016) 2.2 (2017)	89/10 (2015) 87/12 (2016) 84/9 (2017)	1275 1046 388 (2017)	<ul style="list-style-type: none"> <li>• PTES is also used for short-term storage</li> <li>• Lower storage temperature by rational use of heat pump</li> <li>• New liner guaranteed for 20 years when the temperature is &lt;90 °C</li> <li>• The inlet/outlet pipes are made of stainless steel</li> <li>• The pH of water remains at 9.8</li> </ul>		[28,46,149]
Gram	42 % (2016) 37 % (2017)	50 % (2016) 50 % (2017)	0.9 (2016) 0.7 (2017)	84/23(2016) 79/21 (2017)	7650 6463		<ul style="list-style-type: none"> <li>• Large heat loss due to wet insulation</li> <li>• Corrosion inside PTES due to mixing of iron and galvanized metal</li> </ul>	[48]
Vojens	45 %	–	–	80/–	–			[52,164]
Toftlund	>45 %	72 (2020)	–	–	4400 (2018) 2800 (2019)	<ul style="list-style-type: none"> <li>• Excess heat from industry</li> <li>• Leca is used as the insulation layer of the cover</li> </ul>		[54,163]

(continued on next page)

**Table 7 (continued)**

Project	Solar fraction	Storage efficiency	Number of storage cycles	Storage max/min temperature (°C)	Storage heat loss (MWh)	Success experience	Failure experience	References
Langkazi Tibet	>90 %	-	-	-	-	<ul style="list-style-type: none"> <li>A special liner that can withstand temperatures above 90 °C for a long time is used</li> <li>Successful use in harsh weather conditions</li> </ul>	<ul style="list-style-type: none"> <li>Heat loss in the first year of operation is 84 % higher than the design value</li> <li>Energy waste due to system matching problems</li> </ul>	[57]

**Fig. 27.** Comparison of performance metrics [11,31,32,38,46,48,52,54,57,141,144,147,161–164].

- The design and construction of the floating cover remain the biggest challenge in PTES construction as it generates the most considerable heat loss and accounts for a large portion of the investment. Additionally, the reliability and durability of the thermal insulation and lining materials are critical for such massively buried PTES in a high-temperature environment as several projects must be shut down to repair the damaged floating cover.
- At present, the accuracy of PTES numerical approaches is insufficient, especially the prediction deviation of heat loss, PTES temperature, and soil temperature is still significant. In some cases, PTES temperature deviation inside PTES can be as high as 14 K, and the heat loss to the side walls is always grossly overestimated.

This paper contributes to a certain extent to deepen the understanding of the development and the challenges of PTES. Future research should concentrate on the following investigations:

- Considerably more work needs to be done to develop a reliable cover design and construction methods to maintain stability for long-term applications. Ongoing research needs to expand the knowledge of insulation and liner materials from multiple dimensions, such as physical properties in different physical environments, lifetime, cost, and installing method.
- It would be interesting to assess the effects of different inlet/outlet designs on the thermal performance of large-scale PTES as the current design of the inlet/outlet diffuser draws on the experience of small-scale energy storage.
- Groundwater is considered one of the important factors affecting the performance of PTES. Better modeling of the groundwater will help us achieve a higher degree of accuracy by the simulation models.
- Combining the advantages of different platforms of PTES models to build a co-simulation platform is intriguing and should be future explored. Furthermore, system modeling is considered necessary to

integrate PTES in the energy system with different system structures and operation strategies.

#### Declaration of competing interest

The authors declare that they have no known competing financial interests or personal relationships that could have appeared to influence the work reported in this paper.

#### Data availability

Data will be made available on request.

#### Acknowledgments

The work is partly funded by the Danish Energy Agency EUDP project (no. 64020-2036) and the Chinese Scholarship Council (CSC). Without their support, the research would not be possible.

#### References

- [1] IEA, Heating, IEA, Paris. <https://www.iea.org/reports/heating>, 2020.
- [2] F. Mauthner, S. Herkel, in: Technology and Demonstrators - Technical Report Subtask C - Part C1, 2016, pp. 1–31. [http://task52.iea-shc.org/data/sites/1/publications/IEA-SHC-Task52-STC1-Classification-and-benchmarking-Report-2\\_016-03-31.pdf](http://task52.iea-shc.org/data/sites/1/publications/IEA-SHC-Task52-STC1-Classification-and-benchmarking-Report-2_016-03-31.pdf).
- [3] W. Weiss, M. Spörk-Dür, Solar heat worldwide - global market development and trends in 2019 / detailed market figures. <https://www.iea-shc.org/Data/Sites/1/publications/Solar-Heat-Worldwide-2020.pdf>, 2018.
- [4] D. Tschopp, Z. Tian, M. Berberich, J. Fan, B. Perers, S. Furbo, Large-scale solar thermal systems in leading countries: a review and comparative study of Denmark, China, Germany and Austria, Appl. Energy 270 (2020) 1–31, <https://doi.org/10.1016/j.apenergy.2020.114997>.
- [5] J. Xu, R.Z. Wang, Y. Li, A review of available technologies for seasonal thermal energy storage, Sol. Energy 103 (2014) 610–638, <https://doi.org/10.1016/j.solener.2013.06.006>.
- [6] G. Alva, Y. Lin, G. Fang, An overview of thermal energy storage systems, Energy 144 (2018) 341–378, <https://doi.org/10.1016/j.energy.2017.12.037>.

- [7] C. Ann Cruickshank, C. Baldwin, Sensible thermal energy storage: diurnal and seasonal, *Storing Energy* (2016) 291–311, <https://doi.org/10.1016/B978-0-12-803440-8.00015-4>.
- [8] D. Olsthoorn, F. Haghhighat, P.A. Mirzaei, Integration of storage and renewable energy into district heating systems: a review of modelling and optimization, *Sol. Energy* 136 (2016) 49–64, <https://doi.org/10.1016/j.solener.2016.06.054>.
- [9] M.N. Fisch, M. Guigas, J.O. Dalenbäck, A review of large-scale solar heating systems in Europe, *Sol. Energy* 63 (1998) 355–366, [https://doi.org/10.1016/S0038-092X\(98\)00103-0](https://doi.org/10.1016/S0038-092X(98)00103-0).
- [10] Planenergi, in: Best practice for implementation and operation of large scale borehole and pit heat thermal storage, 2019, pp. 1–22, <https://www.solar-district-heating.eu/wp-content/uploads/2019/10/Best-practice-Br%C3%A6strup-Marstal-Dronninglund-and-Gram-003.pdf>.
- [11] D. Bauer, R. Marx, J. Nußbicker-Lux, F. Ochs, W. Heidemann, H. Müller-Steinhagen, German central solar heating plants with seasonal heat storage, *Sol. Energy* 84 (2010) 612–623, <https://doi.org/10.1016/j.solener.2009.05.013>.
- [12] D. Mangold, T. Schmidt, The next generations of seasonal thermal energy storage in Germany 8 (2009).
- [13] T. Yang, W. Liu, G.J. Kramer, Q. Sun, Seasonal thermal energy storage: a techno-economic literature review, *Renew. Sust. Energ. Rev.* 139 (2021), 110732, <https://doi.org/10.1016/j.rser.2021.110732>.
- [14] C. Bott, I. Dressel, P. Bayer, State-of-technology review of water-based closed seasonal thermal energy storage systems, *Renew. Sust. Energ. Rev.* 113 (2019), 109241, <https://doi.org/10.1016/j.rser.2019.06.048>.
- [15] F. Ochs, A. Dahash, A. Tosato, Janetti M. Bianchi, Techno-economic planning and construction of cost-effective large-scale hot water thermal energy storage for renewable district heating systems, *Renew. Energy* 150 (2020) 1165–1177, <https://doi.org/10.1016/j.renene.2019.11.017>.
- [16] E. Guelpa, V. Verda, Thermal energy storage in district heating and cooling systems: A review, *Appl. Energy* 252 (2019), 113474, <https://doi.org/10.1016/j.apenergy.2019.113474>.
- [17] U. Pelay, L. Luo, Y. Fan, D. Stitou, M. Rood, Thermal energy storage systems for concentrated solar power plants, *Renew. Sust. Energ. Rev.* 79 (2017) 82–100, <https://doi.org/10.1016/j.rser.2017.03.139>.
- [18] I. Sarbu, C. Sebarchievici, A comprehensive review of thermal energy storage, *Sustainability* 10 (2018) 191, <https://doi.org/10.3390/su10010191>.
- [19] G. Li, Sensible heat thermal storage energy and exergy performance evaluations, *Renew. Sust. Energ. Rev.* 53 (2016) 897–923, <https://doi.org/10.1016/j.rser.2015.09.006>.
- [20] T. Chmidt, T. Pauschinger, P.A. Sørensen, A. Snijders, R. Djebbar, R. Boultier, et al., Design aspects for large-scale pit and aquifer thermal energy storage for district heating and cooling, *Energy Procedia* 149 (2018) 585–594, <https://doi.org/10.1016/j.egypro.2018.08.223>.
- [21] H. Mahon, D. O'Connor, D. Friedrich, B. Hughes, A review of thermal energy storage technologies for seasonal loops, *Energy* 239 (2022), 122207, <https://doi.org/10.1016/j.energy.2021.122207>.
- [22] A.V. Novo, J.R. Bayon, D. Castro-Fresno, J. Rodriguez-Hernandez, Review of seasonal heat storage in large basins: water tanks and gravel-water pits, *Appl. Energy* 87 (2010) 390–397, <https://doi.org/10.1016/j.apenergy.2009.06.033>.
- [23] X. Zhou, Y. Xu, X. Zhang, D. Xu, Y. Linghu, H. Guo, et al., Large scale underground seasonal thermal energy storage in China, *J. Energy Storage* 33 (2021), 102026, <https://doi.org/10.1016/j.est.2020.102026>.
- [24] A. Dahash, F. Ochs, M.B. Janetti, W. Streicher, Advances in seasonal thermal energy storage for solar district heating applications: A critical review on large-scale hot-water tank and pit thermal energy storage systems, *Appl. Energy* 239 (2019) 296–315, <https://doi.org/10.1016/j.apenergy.2019.01.189>.
- [25] Planenergi, in: Design of the pit heat storage of the demonstration plant at Marstal fjernvarme, 2013, pp. 1–19.
- [26] C. Chang, B. Nie, G. Leng, C. Li, X. She, X. Peng, et al., Influences of the key characteristic parameters on the thermal performance of a water pit seasonal thermal storage, *Energy Procedia* 142 (2017) 495–500, <https://doi.org/10.1016/j.egypro.2017.12.077>.
- [27] F. Ochs, J. Nußbicker, R. Marx, H. Koch, W. Heidemann, H. Müller-Steinhagen, Solar assisted district heating system with seasonal thermal energy storage in Eggenstein-Leopoldshafen, EuroSun, Lisboa, 2008.
- [28] A. Sørensen, T. Schmidt, Design and construction of large scale heat storages for district heating in Denmark, in: 14th International Conference on Energy Storage, 2018, Turkey.
- [29] C. Chang, G. Leng, C. Li, B. Nie, X. She, X. Peng, et al., Investigation on transient cooling process in a water heat storage tank with inclined sidewalls, *Energy Procedia* 142 (2017) 142–147, <https://doi.org/10.1016/j.egypro.2017.12.023>.
- [30] F. Ochs, W. Heidemann, H. Müller-Steinhagen, Seasonal thermal energy storage: a challenging application for geosynthetics, in: 4th European Geosynthetics Conference, 2008, 105.
- [31] G.K. Pavlov, B.W. Olesen, Seasonal ground solar thermal energy storage - review of systems and applications, in: 30th ISES Biennial Solar World Congress 6, 2011, pp. 4864–4874, <https://doi.org/10.18086/swc.2011.29.24>.
- [32] E. Hahne, ITW solar heating system: An oldtimer fully in action, *Sol. Energy* 69 (2000) 469–493, [https://doi.org/10.1016/S0038-092X\(00\)00115-8](https://doi.org/10.1016/S0038-092X(00)00115-8).
- [33] M. Hornberger, N. Fisch, E. Hahne, Solar assisted low temperature heating system with seasonal storage, in: W.H. blass (Ed.), *Advances In Solar Energy Technology*, Institute of Physical Electronics, University of Stuttgart, Germany, 1988, pp. 1282–1287.
- [34] F. Ochs, W. Heidemann, H. Koch, Erdreich / wasser-erdbecken-wärmespeicher mit direktem beladesystem, in: OTTI 16. Symposium Thermische Solarenergie, Stuttgart, 2006, pp. 88–93. <https://elib.dlr.de/45161/>.
- [35] T. Schmidt, D. Mangold, H. Müller-Steinhagen, Seasonal thermal energy storage in Germany, in: ISES Solar World Congress, 2003, pp. 1–7.
- [36] M. Guadalfajara, M.A. Lozano, L.M. Serra, Analysis of large thermal energy storage for solar district heating, Eurotherm Seminar #99 Advances in Thermal Energy Storage (2014) 1–10, <https://doi.org/10.13140/2.1.3857.6008>.
- [37] F. Ochs, W. Heidemann, H. Koch, Soil-water pit heat store with direct charging system - Technology and Economy, EuroSun, United Kingdom, 2006.
- [38] M. Bodmann, H. Koch, M. Pfeil, Solare nahwärmeversorgung mit kies / wasserwärmespeicher in Steinfurt-Borghorst, <https://www.tu-braunschweig.de/index.php?eID=download&t=f&f=30209&token=ebaebef0a2f25a0f30ea24a15a63150c82f5507>, 1998.
- [39] D. Bauer, R. Marx, H. Drück, Solar district heating for the built environment technology and future trends within the european project Einstein, *Energy Procedia* 57 (2014) 2716–2724, <https://doi.org/10.1016/j.egypro.2014.10.303>.
- [40] BINE informationsdienst. School refurbishment combined with local solar heating. <https://api.deutsche-digitale-bibliothek.de/binary/41b6cd75-2ed6-4379-923e-56b4d3df3f92.pdf>.
- [41] L. Jensen, D. Rutz, C. Doczekal, V. Gjorgievski, I. Batas-Bjelic, A. Kazagic, et al., Best practice examples of renewable district heating and cooling. Market uptake of small modular renewable district heating and cooling grids for communities. [https://www.coolheating.eu/images/downloads/DO2.1\\_Best\\_Practice.pdf](https://www.coolheating.eu/images/downloads/DO2.1_Best_Practice.pdf), 2016.
- [42] J. Fan, J. Huang, O.L. Andersen, S. Furbo, Thermal performance analysis of a solar heating plant, in: ISES Solar World Congress, 2017, <https://doi.org/10.18086/swc.2017.06.05>. Abu Dhabi, United Arab Emirates.
- [43] B. Epp, Seasonal pit heat storage: cost benchmark of 30 EUR/m<sup>3</sup>. <https://solarthermalworld.org/news/seasonal-pit-heat-storage-cost-benchmark-30-eurm3>, 2019.
- [44] M.V. Jensen, Seasonal pit heat storages - Guidelines for materials & construction. IEA - SHC TECH SHEET 45 2014;1-31. <http://task45.iea-shc.org/data/sites/1/p/publications/IEA-SHC%20T45.B.3.2%20TECH%20Seasonal%20storages%20-%20Water%20Pit%20Guidelines.pdf>.
- [45] Danish District Heating Association, PlanEnergi. Solar district heating - inspiration and experiences from Denmark. <http://task55.iea-shc.org/Data/Site1/publications/SDH%20Inspiration%20Experience%20DK%20v5.pdf>, 2018.
- [46] C. Winterscheid, Dronninglund district heating monitoring data evaluation for the years 2015–2017. [https://www.solar-district-heating.eu/wp-content/uploads/2019/10/Dronninglund-evaluation-report-2015-2017\\_20190531.pdf](https://www.solar-district-heating.eu/wp-content/uploads/2019/10/Dronninglund-evaluation-report-2015-2017_20190531.pdf), 2017.
- [47] B. Epp, Denmark: Dronninglund inaugurates 26 MWth solar district heating plant 6, 2014. <https://www.solarthermalworld.org/news/denmark-dronninglund-inaugurates-26-mwth-solar-district-heating-plant>.
- [48] C. Winterscheid, Gram district heating monitoring data evaluation for the years 2016–2017. [https://www.solar-district-heating.eu/wp-content/uploads/2019/10/Gram-evaluation-report-2016-2017\\_20190531.pdf](https://www.solar-district-heating.eu/wp-content/uploads/2019/10/Gram-evaluation-report-2016-2017_20190531.pdf), 2019.
- [49] PlanEnergi, A presentation of the Danish pit and borehole thermal energy storages in Bræstrup, Marstal, Dronninglund and Gram. [https://ens.dk/sites/en.s.dk/files/Forsknings\\_og\\_udvikling/sol\\_til\\_fjernvarme\\_brochure\\_endelig.pdf](https://ens.dk/sites/en.s.dk/files/Forsknings_og_udvikling/sol_til_fjernvarme_brochure_endelig.pdf), 2019.
- [50] Ramboll. Heat pumps : the future of district heating?.
- [51] B. Epp, Denmark 37 MW field with 203.000 m<sup>3</sup> storage underway 8 (2014). <https://www.solarthermalworld.org/news/denmark-37-mw-field-203000-m3-storage-underway>.
- [52] Ramboll, World largest thermal heat storage pit in Vojens. <https://stateofgreen.com/en/partners/ramboll/solutions/world-largest-thermal-pit-storage-in-vojen-s/>.
- [53] D. Ved, T. Fjernvarme, Large fyldes med 70.000 kubikmeter varmt vand. <https://jv.dk/artikel/lager-fyldes-med-70-000-kubikmeter-varmt-vand>, 2017.
- [54] Ramboll, Toftlund fjernvarme udvidelse solvarme project, 2015.
- [55] Pedersen MBS, Energilager tager form i Toftlund. [https://www.energy-supply.dk/article/view/341832/energilager\\_tager\\_form\\_i\\_toftlund](https://www.energy-supply.dk/article/view/341832/energilager_tager_form_i_toftlund), 2017.
- [56] Solar district heating, Solar district heating on the roof of the world. <https://www.solar-district-heating.eu/solar-district-heating-on-the-roof-of-the-world/>, 2018.
- [57] Q. Jiao, S. Li, F. Gao, W. Wang, K. Qin, The performance of a high altitude and high solar fraction large-scale district heating project, in: ISES Solar World Congress, International Solar Energy Society, 2019, pp. 459–469.
- [58] Asian Development Bank, Solar district heating in the People's Republic of China status and development potential. <https://www.adb.org/sites/default/files/publication/514916/solar-district-heating-peoples-republic-china.pdf>, 2019.
- [59] L.J. Shah, S. Furbo, Entrance effects in solar storage tanks, *Sol. Energy* 75 (2003) 337–348, <https://doi.org/10.1016/j.solener.2003.04.002>.
- [60] S. Furbo, Hot Water Tanks for Solar Heating Systems, 2004.
- [61] Y. Deng, D. Sun, M. Niu, B. Yu, R. Bian, Performance assessment of a novel diffuser for stratified thermal energy storage tanks - the nonequal-diameter radial diffuser, *J. Energy Storage* 35 (2021), <https://doi.org/10.1016/j.est.2021.102276>.
- [62] J.D. Chung, S.H. Cho, C.S. Tae, H. Yoo, The effect of diffuser configuration on thermal stratification in a rectangular storage tank, *Renew. Energy* 33 (2008) 2236–2245, <https://doi.org/10.1016/j.renene.2007.12.013>.
- [63] P. Fagerlund Carlsson, Temperaturstratificering i varmelagre, Technical University of Denmark, Department of Civil Engineering, 1995.
- [64] I.J. Moncho-Esteve, M. Gasque, P. González-Altozano, G. Palau-Salvador, Simple inlet devices and their influence on thermal stratification in a hot water storage tank, *Energy Build.* 150 (2017) 625–638, <https://doi.org/10.1016/j.enbuild.2017.06.012>.
- [65] E. García-Marí, M. Gasque, R.P. Gutierrez-Colomer, F. Ibáñez, P. González-Altozano, A new inlet device that enhances thermal stratification during charging in a hot water storage tank, *Appl. Therm. Eng.* 61 (2013) 663–669, <https://doi.org/10.1016/j.aplthermaleng.2013.08.023>.

- [66] M.R. Assari, H. Basirat Tabrizi, M. Savadkohy, Numerical and experimental study of inlet-outlet locations effect in horizontal storage tank of solar water heater, *Sustain. Energy Technol. Assess.* 25 (2018) 181–190, <https://doi.org/10.1016/j.seta.2017.12.009>.
- [67] F. Findeisen, T. Urbaneck, B. Platzter, Radial diffusers - simulation of three-dimensional flow effects with CFD (Part 1), *Chem. Ing. Tech.* 90 (2018) 956–968, <https://doi.org/10.1002/cite.201700023>.
- [68] F. Findeisen, T. Urbaneck, B. Platzter, Radial diffusers - simulation of three-dimensional flow effects with CFD (Part 2), *Chem. Ing. Tech.* 90 (2018) 969–978, <https://doi.org/10.1002/cite.201700070>.
- [69] F. Findeisen, T. Urbaneck, B. Platzter, Radial diffusers - simulation of three-dimensional flow effects with CFD (Part 3), *Chem. Ing. Tech.* 90 (2018) 1065–1072, <https://doi.org/10.1002/cite.201700126>.
- [70] F. Findeisen, U. Kroll, T. Urbaneck, B. Platzter, Radial diffusers in stratified hot water stores: Econtry optimization with CFD, in: ISES Solar World Congress, 2017, pp. 726–734, <https://doi.org/10.18086/swc.2017.13.04>.
- [71] PlanEnergi, Niras, in: Dronninglund solar thermal plant, 2014, pp. 1–12. [https://www.dronninglundfjernvarme.dk/media/2984/brochure\\_dronninglund\\_2015\\_booklet\\_eng\\_web.pdf](https://www.dronninglundfjernvarme.dk/media/2984/brochure_dronninglund_2015_booklet_eng_web.pdf).
- [72] Underground Thermal Energy Storage (UTES) - state - of - the - art, example cases and lessons learned, in: A.J. Kallese, T. Vangkilde-Pedersen (Eds.), *HEATSTORE project report, GEOTHERMICA-ERA NET Cofund Geothermal*, 2019, 130 pp + appendices.
- [73] F. Ochs, W. Heidemann, H. Müller-Steinhagen, Performance of large-scale seasonal thermal energy stores, *J. Sol. Energy Eng.* 131 (2009), 041005, <https://doi.org/10.1115/1.3197842>.
- [74] K. Ellehaug, T.E. Pedersen, Solar heat storages in district heating networks. <https://www.osti.gov/etdweb/servlets/purl/928828>, 2007.
- [75] Saint-Gobain Weber A/S, Weber leverer isolerende dyne til verdens største damvarmelager 11, 2015.
- [76] PlanEnergi, Sunstore 3 phase 2 implementation. <http://planenergi.dk/wp-content/uploads/2018/05/26-Sunstore-3-Final-report.pdf>, 2015.
- [77] PlanEnergi, Summary technical description of the sunstore 4 plant in Marstal. <https://www.solarmarstal.dk/media/6600/summary-technical-description-marsatal.pdf>, 2013.
- [78] Aalborg CSP. Pit thermal energy storage (PTES). <https://www.aalborgcsp.com/business-areas/thermal-energy-storage-tes/pit-thermal-energy-storage-ptes/>.
- [79] Aalborg CSP, Aalborg CSP improves bankability of thermal storage technology with certificate from Lloyd's register for unique lid technology.. <https://www.aalborgcsp.com/news-events/newsletter/news/aalborg-csp-improves-bankability-of-thermal-storage-technology/>, 2021.
- [80] K. Weinhold, T. Werner, S. Grob, S. Helffritsch, D. Haas, Green Heat<sup>3</sup> Entwicklung innovativer Energieversorgungstechniken und -strukturen mit den Kernkomponenten modularer Großwärmespeicher und Maxianlage Solarthermie. [https://tu-dresden.de/ing/maschinewesen/iet/gewv/ressourcen/dateien/forschung\\_und\\_projekte/projekte/20220\\_Endbericht\\_GH3\\_freigegeben.pdf?lang=en](https://tu-dresden.de/ing/maschinewesen/iet/gewv/ressourcen/dateien/forschung_und_projekte/projekte/20220_Endbericht_GH3_freigegeben.pdf?lang=en), 2019.
- [81] F. Ochs, W. Heidemann, H. Müller-Steinhagen, Effective thermal conductivity of moistened insulation materials as a function of temperature, *Int. J. Heat Mass Transf.* 51 (2008) 539–552, <https://doi.org/10.1016/j.ijheatmasstransfer.2007.05.005>.
- [82] F. Ochs, W. Heidemann, H. Müller-Steinhagen, Effective thermal conductivity of the insulation of high temperature underground thermal stores during operation, 2006, pp. 1–7.
- [83] A. Abdou, I. Budaiwi, The variation of thermal conductivity of fibrous insulation materials under different levels of moisture content, *Constr. Build. Mater.* 43 (2013) 533–544, <https://doi.org/10.1016/j.conbuildmat.2013.02.058>.
- [84] W. Villasmil, L.J. Fischer, J. Wortscheck, A review and evaluation of thermal insulation materials and methods for thermal energy storage systems, *Renew. Sust. Energ. Rev.* 103 (2019) 71–84, <https://doi.org/10.1016/j.rser.2018.12.040>.
- [85] D. Mangold, L. Deschaire, Seasonal thermal energy storage - report on state of the art and necessary further R + D, in: IEA-SHC Task 45 Large Systems, 2015, pp. 1–48. [http://task45.iea-shc.org/data/sites/1/publications/IEA\\_SHC\\_Task45\\_B\\_Report.pdf](http://task45.iea-shc.org/data/sites/1/publications/IEA_SHC_Task45_B_Report.pdf).
- [86] E.A. Yatsenko, B.M. Goltsman, V.A. Smolny, A.S. Kosarev, Investigation of a porous structure formation mechanism of a foamed slag glass based on the glycerol foaming mixture, *Res. J. Pharm. Biol. Chem. Sci.* 7 (2016) 1073–1081.
- [87] A. Zukri, R. Nazir, K.N.M. Said, H. Moayedi, Physical and mechanical properties of lightweight expanded clay aggregate (LECA), in: MATEC Web of Conferences, 2018, p. 250, <https://doi.org/10.1051/matecconf/201825001016>.
- [88] M. Bianchi Janetti, T. Plaz, F. Ochs, O. Klesnil, W. Feist, Thermal conductivity of foam glass gravels: a comparison between experimental data and numerical results, *Energy Procedia* 78 (2015) 3258–3263, <https://doi.org/10.1016/j.egypro.2015.11.713>.
- [89] F. Ochs, in: Temperature and moisture dependence of the thermal conductivity of insulation materials, 2005, pp. 1–5. <http://wevik.hu/file/lambdavaltozas2.pdf>.
- [90] B.P. Jelle, Traditional, state-of-the-art and future thermal building insulation materials and solutions - properties, requirements and possibilities, *Energy Build.* 43 (2011) 2549–2563, <https://doi.org/10.1016/j.enbuild.2011.05.015>.
- [91] NMC, Nomalen 28N, NMC Termonova Oy. <https://dms.etrta.fi:9900/72192/conversions/original?version=0>, 2015.
- [92] H. Kim, D. Park, E.S. Park, H.M. Kim, Numerical modeling and optimization of an insulation system for underground thermal energy storage, *Appl. Therm. Eng.* 91 (2015) 687–693, <https://doi.org/10.1016/j.aplthermaleng.2015.08.070>.
- [93] Z. Ademović, J. Suljagić, Zulić J. Zahida, Ademović, et al., Influence of physical properties on thermal conductivity of polystyrene insulation materials, *Contemp. Mater.* 1 (2017) 42–47, <https://doi.org/10.7251/COMEN1701042A>.
- [94] J. Luis, P. Ordóñez, Characterization of mussel shells as a bio-based building insulation material, in: 3rd International Conference on Bio-based Building Materials 37, 2019, pp. 525–531, <https://doi.org/10.26168/icbbm2019.76>.
- [95] M.K. Grabmann, G.M. Wallner, W. Buchberger, D. Nitsche, Aging and lifetime assessment of polyethylene liners for heat storages - effect of liner thickness, in: ISES Solar World Congress, 2017, pp. 753–760, <https://doi.org/10.18086/swc.2017.13.07>.
- [96] M. Koehl, M. Meir, P. Papillon, G. Wallner, S. Sandrin, Polymeric materials for solar thermal applications, 2015, <https://doi.org/10.1002/9783527659609>.
- [97] J. Scheirs, *A Guide to Polymeric Geomembranes: A Practical Approach*, Wiley, 2009, United States.
- [98] R. Kübler, N. Fisch, E. Hahne, High temperature water pit storage projects for the seasonal storage of solar energy, *Sol. Energy* 61 (1997) 97–105, [https://doi.org/10.1016/S0038-092X\(97\)00040-6](https://doi.org/10.1016/S0038-092X(97)00040-6).
- [99] KAT, Experimental investigation of possible use of hdpe as thermal storage material in thermal storage type solar cookers, *Int. J. Res. Eng. Technol. Sci.* 04 (2015) 92–99, <https://doi.org/10.15623/ijret.2015.042019>.
- [100] A. Patti, D. Acierno, Thermal Conductivity of Polypropylene-based Materials, in: W. Wang, Y. Zeng (Eds.), *Polypropylene Polymerization and Characterization of Mechanical and Thermal Properties*, 2019, IntechOpen.
- [101] M.K. Grabmann, G.M. Wallner, K. Grabmayer, D. Nitsche, R.W. Lang, Aging behavior and lifetime assessment of polyolefin liner materials for seasonal heat storage using micro-specimen, *Sol. Energy* 170 (2018) 988–990, <https://doi.org/10.1016/j.solener.2018.06.046>.
- [102] Polyethylene - Low density ( LDPE ) material information. <https://www.goodfellow.com/E/Polyethylene-Low-Density.html>.
- [103] W.V. Titow, *PVC Technology, (Fourth Edition)*, Elsevier Applied Science Publ., 1984, USA.
- [104] L.W. McKeen, 11 - Elastomers and rubbers, in: *The Effect of Long Term Thermal Exposure on Plastics and Elastomers*, William Andrew Publishing, Norwich, NY, 2014, pp. 239–271, <https://doi.org/10.1016/B978-0-323-22108-5.00011-4>.
- [105] A. Ma, X. Wang, Y. Chen, J. Yu, W. Zheng, Y. Zhao, Largely enhanced thermal conductivity of ethylene-propylene-diene monomer composites by addition of graphene ball, *Compos. Commun.* 13 (2019) 119–124, <https://doi.org/10.1016/j.coco.2019.04.005>.
- [106] M. Gasque, P. González-Altozano, D. Maurer, I.J. Moncho-Esteve, R.P. Gutiérrez-Colomer, G. Palau-Salvador, et al., Study of the influence of inner lining material on thermal stratification in a hot water storage tank, *Appl. Therm. Eng.* 75 (2015) 344–356, <https://doi.org/10.1016/j.aplthermaleng.2014.10.040>.
- [107] J. Carvill, 3 - Thermodynamics and heat transfer, in: *Mechanical Engineer's Data Handbook* Butterworth-Heinemann, 1993, pp. 102–145.
- [108] F. Ochs, A. Dahash, A. Tosatto, M. Reisenbichler, K. O'Donovan, G. Gauthier, et al., Comprehensive comparison of different models for large-Scale thermal energy storage, in: Proceedings of the International Renewable Energy Storage Conference 2021 (IRES 2021) 8, 2022, pp. 36–51, <https://doi.org/10.2991/ahe.k.220301.005>.
- [109] P. Sorknaes, Simulation method for a pit seasonal thermal energy storage system with a heat pump in a district heating system, *Energy* 152 (2018) 533–538, <https://doi.org/10.1016/j.energy.2018.03.152>.
- [110] X. Pan, Y. Xiang, M. Gao, J. Fan, S. Furbo, D. Wang, et al., Long-term thermal performance analysis of a large-scale water pit thermal energy storage, *J. Energy Storage* 52 (2022), 105001, <https://doi.org/10.1016/j.est.2022.105001>.
- [111] G. Gauthier, Benchmarking and improving models of subsurface heat storage dynamics, comparison of Danish PTES and BTES installation measurements with their corresponding TRNSYS models. [https://www.heatstore.eu/documents/H\\_EATSTORE\\_WP2\\_D2.3-Danish%20PTES%20and%20BTES%20installations\\_Fina1.2020.11.02.pdf](https://www.heatstore.eu/documents/H_EATSTORE_WP2_D2.3-Danish%20PTES%20and%20BTES%20installations_Fina1.2020.11.02.pdf), 2020.
- [112] Z. Xie, Y. Xiang, D. Wang, O. Kusyy, W. Kong, S. Furbo, et al., Numerical investigations of long-term thermal performance of a large water pit heat storage, *Sol. Energy* 224 (2021) 808–822, <https://doi.org/10.1016/j.solener.2021.06.027>.
- [113] K. Narula, Filho F. de Oliveira, W. Villasmil, M.K. Patel, Simulation method for assessing hourly energy flows in district heating system with seasonal thermal energy storage, *Renew. Energy* 151 (2020) 1250–1268, <https://doi.org/10.1016/j.renene.2019.11.121>.
- [114] K. Kubinski, Ł. Szablowski, Dynamic model of solar heating plant with seasonal thermal energy storage, *Renew. Energy* 145 (2020) 2025–2033, <https://doi.org/10.1016/j.renene.2019.07.120>.
- [115] Y. Bai, M. Yang, J. Fan, X. Li, L. Chen, G. Yuan, et al., Influence of geometry on the thermal performance of water pit seasonal heat storages for solar district heating, *Build. Simul.* (2020), <https://doi.org/10.1007/s12273-020-0671-9>.
- [116] Y. Bai, Z. Wang, J. Fan, M. Yang, X. Li, L. Chen, et al., Numerical and experimental study of an underground water pit for seasonal heat storage, *Renew. Energy* 150 (2020) 487–508, <https://doi.org/10.1016/j.renene.2019.12.080>.
- [117] A. Dahash, F. Ochs, A. Tosatto, W. Streicher, Toward efficient numerical modeling and analysis of large-scale thermal energy storage for renewable district heating, *Appl. Energy* 279 (2020), 115840, <https://doi.org/10.1016/j.apenergy.2020.115840>.
- [118] A. Dahash, M.B. Janetti, F. Ochs, Numerical analysis and evaluation of large - scale hot water tanks and pits in district heating systems, in: 16th IBPSA International Conference and Exhibition, 2019, <https://doi.org/10.26868/25222708.2019.210566>, Rome, Italy.

- [119] X. Li, Z. Wang, J. Li, M. Yang, G. Yuan, Y. Bai, et al., Comparison of control strategies for a solar heating system with underground pit seasonal storage in the non-heating season, *J. Energy Storage* 26 (2019), 100963, <https://doi.org/10.1016/j.est.2019.100963>.
- [120] P. Nageler, G. Schweiger, H. Schranzhofer, R. Heimrath, T. Mach, L.M. Fochler, et al., Co-simulation workflow for the dynamic modelling and simulation of large-scale district energy systems institute of thermal engineering, in: 16th IBPSA international conference and exhibition, 2019, <https://doi.org/10.26868/25222708.2019.211048>. Rome, Italy.
- [121] A. Dahash, M.B. Janetti, F. Ochs, M. Science, Detailed 3-D models of a large-scale underground thermal energy storage with consideration of groundwater conditions, in: International Sustainable Energy Conference, 2018, pp. 597–604. Graz, Austria.
- [122] C. Chang, Z. Wu, H. Navarro, C. Li, G. Leng, X. Li, et al., Comparative study of the transient natural convection in an underground water pit thermal storage, *Appl. Energy* 208 (2017) 1162–1173, <https://doi.org/10.1016/j.apenergy.2017.09.036>.
- [123] J. Fan, J. Huang, A. Chatzidiakos, S. Furbo, Experimental and theoretic investigations of thermal behavior of a seasonal water pit heat storage, in: ISES Solar World Congress, 2017, pp. 714–725, <https://doi.org/10.18086/swc.2017.13.03>.
- [124] A. Chatzidiakos, CFD calculations for solar water pond heat storages, Technical University of Denmark, 2016.
- [125] P. Reiter, H. Poier, C. Holter, BIG Solar Graz: solar district heating in Graz - 500,000 m<sup>2</sup> for 20% solar Fraction, *Energy Procedia* 91 (2016) 578–584, <https://doi.org/10.1016/j.egypro.2016.06.204>.
- [126] F. Ochs, Large-scale thermal energy stores in district heating systems - simulation based optimization, 2014, <https://doi.org/10.18086/eurosun.2014.19.09>. EuroSun 2014, France.
- [127] S. Raab, D. Mangold, H. Müller-Steinhagen, Validation of a computer model for solar assisted district heating systems with seasonal hot water heat store, *Sol. Energy* 79 (2005) 531–543, <https://doi.org/10.1016/j.solener.2004.10.014>.
- [128] E. Yamaguchi, Finite element method, in: Bridge Engineering Handbook: Fundamentals, Second Edition, 2014, pp. 225–251, <https://doi.org/10.1201/b15616>.
- [129] A. Dahash, M.B. Janetti, F. Ochs, Detailed axial symmetrical model of large - scale underground thermal energy storage, in: COMSOL 2018 Conference, 2018. Lausanne, Switzerland.
- [130] D. Rutz, C. Winterscheid, T. Pauschinger, S. Grimm, T. Roth, B. Doračić, et al., Upgrading the performance of district heating networks, in: WIP Renewable Energies, Munich, Germany, 2019, [https://www.upgrade-dh.eu/images/Publications%20and%20Reports/D2.5\\_2019-07-02\\_Ugrade-DH\\_Handbook\\_EN.pdf](https://www.upgrade-dh.eu/images/Publications%20and%20Reports/D2.5_2019-07-02_Ugrade-DH_Handbook_EN.pdf).
- [131] A. Dahash, F. Ochs, G. Giuliani, A. Tosatto, Understanding the interaction between groundwater and large-scale underground hot-water tanks and pits, *Sustain. Cities Soc.* 71 (2021), 102928, <https://doi.org/10.1016/j.scs.2021.102928>.
- [132] J.A. Duffie, W.A. Beckman, Solar engineering of thermal processes, *Am. J. Phys.* 53 (1985) 382, <https://doi.org/10.1119/1.14178>.
- [133] L. Mazzarella, S. Holst, Multi-flow stratified thermal storage model with full mixed layers, TRNSYS Version. [https://www.trnsys.de/static/d747464ad7627a47a6610a89da64e9/Type\\_342.en.pdf](https://www.trnsys.de/static/d747464ad7627a47a6610a89da64e9/Type_342.en.pdf), 1992.
- [134] D. Buoro, P. Pinamonti, M. Reini, Optimization of a distributed cogeneration system with solar district heating, *Appl. Energy* 124 (2014) 298–308, <https://doi.org/10.1016/j.apenergy.2014.02.062>.
- [135] K.K. Hansen, P.N. Hansen, Heat storage in an uninsulated water pit: construction and testing of a 500 m<sup>3</sup> store, in: Technical University of Denmark, Department of Civil Engineering, 1983, pp. 404–412, [https://doi.org/10.1007/978-94-009-7924-6\\_54](https://doi.org/10.1007/978-94-009-7924-6_54).
- [136] A. Heller, Floating lid constructions for pit water storage - a survey, in: Technical University of Denmark, Department of Civil Engineering, 1997.
- [137] P.N. Hansen, K.K. Hansen, V. Ussing, Seasonal heat storage in underground warm water pit: design of a 500 m<sup>3</sup> store, in: Technical University of Denmark, Department of Civil Engineering 4, 1984, pp. 490–501.
- [138] A. Heller, in: Development of Seasonal Storage in Denmark: Status of Storage Programme 1997–2000. Terrastock 2000, Proceedings, University of Stuttgart, 2000, pp. 47–52.
- [139] K.K. Hansen, P.N. Hansen, V. Ussing, Seasonal heat storage in underground warm water pit: design of a 30...50.000 m<sup>3</sup> storage, in: Technical University of Denmark, Department of Civil Engineering 4, 1984, pp. 490–501, [https://doi.org/10.1007/978-94-009-6508-9\\_170](https://doi.org/10.1007/978-94-009-6508-9_170).
- [140] F. Ochs, H. Müller-Steinhagen, Abschlussbericht zum vorhaben: weiterentwicklung der Erdbecken-Wärmespeichertechnologie. [https://www.igte.uni-stuttgart.de/veroeffentlichungen/publikationen/publikationen\\_08-05.pdf](https://www.igte.uni-stuttgart.de/veroeffentlichungen/publikationen/publikationen_08-05.pdf), 2008.
- [141] Central solar heating plants with seasonal storage - status report, 6, <http://www.iea-shc.org/Data/Sites/1/publications/Task%207-%20Central%20Solar%20Heating%20Plants%20with%20Seasonal%20Storage-Status%20Report-June%201990.pdf>, 1990.
- [142] J.O. Dalenbäck, T. Jilar, Swedish solar heating with seasonal storage - design, performance and economy, *Int. J. Ambient Energy* 6 (1985) 123–128, <https://doi.org/10.1080/01430750.1985.9675454>.
- [143] F. Ochs, Stand der Technik erdvergraben Wärmespeicher. FFG store4grid. [http://www.aee-now.at/cms/fileadmin/downloads/projekte/store4grid/store4grid\\_stand\\_der\\_technik.pdf](http://www.aee-now.at/cms/fileadmin/downloads/projekte/store4grid/store4grid_stand_der_technik.pdf), 2013.
- [144] F. Ochs, Solar heating system with seasonal storage at the Solar-Campus Juelich, *Sol. Energy* 69 (2000) 525–533, [https://doi.org/10.1016/S0038-092X\(00\)00116-X](https://doi.org/10.1016/S0038-092X(00)00116-X).
- [145] F. Ochs, W. Heidemann, H. Müller-Steinhagen, H. Koch, Soil-water pit heat store with direct charging system, *Geology* (2006) 1–8.
- [146] T. Urbaneck, B. Platzer, U. Schirmer, Advanced monitoring of gravel water storage, in: 9th International Conference on Thermal Energy Storage, 2003. Warschau, Polen.
- [147] T. Urbaneck, U. Schirmer, Central solar heating plant with gravel water storage. Thermal Energy Storage. [http://ptp.irb.hr/upload/mape/solari/08\\_Thorsten\\_Urbaneck\\_CENTRAL\\_SOLAR\\_HEATING\\_PLANT\\_WITH\\_GRAVEL\\_.pdf](http://ptp.irb.hr/upload/mape/solari/08_Thorsten_Urbaneck_CENTRAL_SOLAR_HEATING_PLANT_WITH_GRAVEL_.pdf), 2000.
- [148] T. Schmidt, Monitoring results from large-scale solar thermal plants with long term storage in Marstal, Brædstrup and Dronninglund, Denmark. [https://businesstdbox.com/Green\\_Solutions/66372775-Monitoring-results-from-large-scale-solar-thermal-plants-with-long-term-storage-in-marstal-braedstrup-and-dronninglund-denmark.html](https://businesstdbox.com/Green_Solutions/66372775-Monitoring-results-from-large-scale-solar-thermal-plants-with-long-term-storage-in-marstal-braedstrup-and-dronninglund-denmark.html).
- [149] T. Schmidt, A. Sørensen, Monitoring results from large scale heat storages for district heating in Denmark. 14th International Conference on Energy Storage, Adana, Turkey, [https://planenergi.dk/wp-content/uploads/2018/05/Schmidt-and-Sørensen\\_Monitoring-Results-from-Large-Scale-Heat-storages-.pdf](https://planenergi.dk/wp-content/uploads/2018/05/Schmidt-and-Sørensen_Monitoring-Results-from-Large-Scale-Heat-storages-.pdf), 2018.
- [150] J.E. Nielsen, Solar district heating experiences from Denmark, in: Enegy Platform Workshop 3, Zurich, 2014.
- [151] M. Galindo Fernández, C. Roger-Lacan, U. Gährs, V. Aumaitre, Efficient district heating and cooling systems in the EU - Case studies analysis, replicable key success factors and potential policy implications, EUR 28418 EN, 2016, <https://doi.org/10.2760/371045>.
- [152] Ramboll. Large scale solar water heating and seasonal heat storage pit in Gram. <https://stateofgreen.com/en/partners/ramboll/solutions/large-scale-solar-heating-and-seasonal-heat-storage-pit-in-gram/>.
- [153] R. Marx, D. Bauer, H. Drueck, Energy efficient integration of heat pumps into solar district heating systems with seasonal thermal energy storage, *Energy Procedia* 57 (2014) 2706–2715, <https://doi.org/10.1016/j.egypro.2014.10.302>.
- [154] D. Lindenberger, T. Bruckner, H.M. Groscurth, R. Kümmel, Optimization of solar district heating systems: seasonal storage, heat pumps, and cogeneration, *Energy* 25 (2000) 591–608, [https://doi.org/10.1016/S0360-5442\(99\)00082-1](https://doi.org/10.1016/S0360-5442(99)00082-1).
- [155] M.H. Abokersh, M. Vallès, K. Saikia, L.F. Cabeza, D. Boer, Techno-economic analysis of control strategies for heat pumps integrated into solar district heating systems, *J. Energy Storage* 42 (2021), <https://doi.org/10.1016/j.est.2021.103011>.
- [156] M.H. Abokersh, K. Saikia, L.F. Cabeza, D. Boer, M. Vallès, Flexible heat pump integration to improve sustainable transition toward 4th generation district heating, *Energy Convers. Manag.* 225 (2020), <https://doi.org/10.1016/j.enconman.2020.113379>.
- [157] M. Pinamonti, I. Beausoleil-Morrison, A. Prada, P. Baggio, Water-to-water heat pump integration in a solar seasonal storage system for space heating and domestic hot water production of a single-family house in a cold climate, *Sol. Energy* 213 (2021) 300–311, <https://doi.org/10.1016/j.solener.2020.11.052>.
- [158] R. Yumrutaş, M. Ünsal, Energy analysis and modeling of a solar assisted house heating system with a heat pump and an underground energy storage tank, *Sol. Energy* 86 (2012) 983–993, <https://doi.org/10.1016/j.solener.2012.01.008>.
- [159] Danish Energy Agency, Regulation and planning of district heating in Denmark. [https://ens.dk/sites/ens.dk/files/Globalcooperation/regulation\\_and\\_planning\\_of\\_district\\_heating\\_in\\_denmark.pdf](https://ens.dk/sites/ens.dk/files/Globalcooperation/regulation_and_planning_of_district_heating_in_denmark.pdf), 2016.
- [160] Z. Tian, S. Zhang, J. Deng, J. Fan, J. Huang, W. Kong, et al., Large-scale solar district heating plants in Danish smart thermal grid: Developments and recent trends, *Energy Convers. Manag.* 189 (2019) 67–80, <https://doi.org/10.1016/j.enconman.2019.03.071>.
- [161] J.D. Dalenback, T. Jilar, Swedish solar heating plants with seasonal storage - system design influence on thermal performance and economy, in: First E.C. Conference on Solar Heating, 1984. Amsterdam.
- [162] T. Schemidt, Marstal district heating monitoring data evaluation for the years 2015–2017. [https://www.solar-district-heating.eu/wp-content/uploads/2019/10/Marstal-evaluation-report-2015-2017\\_2019.05.28.pdf](https://www.solar-district-heating.eu/wp-content/uploads/2019/10/Marstal-evaluation-report-2015-2017_2019.05.28.pdf), 2017.
- [163] Ramboll, Pit thermal energy storage update from toftlund. [https://www.heatstorage.eu/documents/20201028\\_DK-temadag\\_Ramb%C3%B8ll%20TES%20project.pdf](https://www.heatstorage.eu/documents/20201028_DK-temadag_Ramb%C3%B8ll%20TES%20project.pdf), 2020.
- [164] District heating with seasonal storage in Vojens Denmark. <https://deepresource.wordpress.com/2020/12/16/district-heating-with-seasonal-storage-in-vojens-denmark/>.
- [165] P.V. Pedersen, O. Mørck, A total energy design for 92 houses with combined use of solar heating and energy conservation, *Energy Conservation in Buildings* (1991) 1–5, <https://doi.org/10.1016/b978-0-08-037215-0.50009-2>.